Chair of Hydrology

Albert-Ludwigs-Universität Freiburg i. Br.

comparing tree species-specific water uptake strategies via continuous *in-situ* monitoring of stable water isotopes

Author:
David Mennekes

Supervisor:
Dr. Orlowski
2 nd Supervisor:
J-Prof. Dr. Hartmann

Thesis for M. Sc. in Hydrology
June 9, 2020

Any fool can know. The point is to understand.

Albert Einstein

Contents

List of Figures

List of Tables

List of Figures in the Appendix

List of Tables in the Appendix

Acknowledgements

I want to thank all those who have contributed to the success of this thesis! Those people are, among others, Natalie, Stefan, Michi, Barbara and Bernhard who helped to set up the experiment, process destructive samples, use *in-situ* isotope probes or discuss results. Furthermore, I want to thank Gesine and Caroline for proofreading my thesis!

Summary

Over the last decades stable water isotopes were established as promising tracer to study soil-tree interactions and root water uptake. Moreover, recently introduced *in-situ* probes are able to measure stable water isotopes in high spatio-temporal resolution within stem xylem tissues and soils. Here, we used an *in-situ* method in a semi-controlled labelling experiment with three 4-6 meter high and 20-year-old coniferous and deciduous trees planted in large pots. By using an *Alnus incana*, a *Pinus pinea* and a *Quercus suber* tree, we expect to cover a wide range of wood and vessel structure as well as different water uptake strategies. Furthermore, we aim for better understanding of influences and behaviour of *in-situ* isotope probes.

In this work, we took advantage of high temporal resolution measurements for tracing the deuterium labelling signal through the soil-plant continuum. Thus, we were able to estimate water travel times from the soils into the xylems derived from isotope tracers. Combining stable water isotope measurements with sap flow velocity, photosynthesis, soil moisture and temperature and soil matrix potential measurements give us the possibility to analyse species specific differences in ecohydrology. Additionally, we tested the *in-situ* measurement method against common used destructive methods during four different measurement campaigns.

Our results show the potential of high temporal resolution stable water isotope probes by measuring almost instant responses of the isotope tracers in the soils. Lower xylem isotope probes (15 cm) capture the arrival of the isotope tracer within one day for *Alnus incana* and *Pinus pinea* while upper xylem isotope probes (150 cm) and xylem probes in *Quercus suber* show a clearly dispersion influenced tracer breakthrough. By using the lower xylem isotope probes we are able to estimate water travel times which are consistent with sap flow velocity measurements. Moreover, our results demonstrate consistent ecohydrological properties among all sensor and probe results in the experiment. Thus, water consumption for *Alnus incana* and *Pinus pinea* is clearly higher than for *Quercus suber* visible through higher water travel velocities and faster drying soils.

We conclude that here used *in-situ* probes seem to capture ecohydrological processes in high temporal resolution. This can be important to better understand hydrological systems and water consumption of trees including temporal water storages, water uptake or loss through tree bark or isotopic fractioning processes within the trees. Better understanding of ecohydrological processes then could help to develop sustainable forest managements under future climatic conditions.

Keywords: ecohydrology, stable water isotopes, plant water uptake, *in-situ* stable water isotope probes, $\delta\ ^{2}H$, $\delta\ ^{18}O$

Zusammenfassung

Stabile Wasserisotope haben sich in den letzten Jahrzehnten zu einem vielversprechenden Tracer für Studien zu Wassersystemen in der Boden-Baum-Interaktion entwickelt. Insbesondere neue *in-situ* Methoden eignen sich gut um stabile Wasserisotope in Böden oder dem Xylem der Bäume in hohen zeitlichen Auflösungen zu messen. Im Rahmen dieser Masterarbeit werden drei verschiedene Baumarten (*Alnus incana*, *Pinus pinea* und *Quercus suber*) eingesetzt, für die, bedingt durch stark variierende Holzstrukturen, eine hohe Variabilität an Wasseraufnahmestrategien erwartet werden darf. Für das Tracerexperiment mit Deuterium wurde die 4 bis 6 Meter hohen und 20 Jahre alten Bäume in große Boxen gepflanzt und die äußerlichen Einflüsse teilweise eingeschränkt.

Mit Hilfe der *in-situ* Isotopensonden kann der Tracer vom Eintritt in die Böden bis zum auftreten im Baumxylem verfolgt werde, wodurch eine Abschätzung der Flusszeiten ermöglicht wird. Des Weiteren können so gewonnene Informationen mit anderen Messungen im Experiment (Sapfluss, Bodenfeuchte, Bodentemperatur, Matrixpotential) verglichen werden, um ökohydrologische Parameter der verschiedenen Baumarten und Wasseraufnahmestrategien abzuleiten. Zusätzlich zu *in-situ*-Messungen wurden noch destruktive Isotopenmessungen vorgenommen, um die Ergebnisse der verschiedenen Methoden zu vergleichen.

Unsere Ergebnisse der Isotopensonden zeigen ein unmittelbares verbreiten des Deuteriumtracers in den Böden, sowie ein Tracerdurchgang innerhalb eines Tages für die unteren Xylemsonden bei *Alnus incana* und *Pinus pinea*. In den oberen Xylemsonden und den Xylemsonden in *Quercus suber* wird dagegen nur ein verzögertes und langsames Ankommen des Tracers gemessen. Vergleicht man jedoch die Fließzeiten des Tracers bis zur unteren Xylemsonde mit dem gemessenen Sapflussgeschwindigkeiten, so ergeben sich größtenteils übereinstimmende Fließgeschwindigkeiten. Auch die anderen gemessenen Boden- und Baumparameter ergänzen sich zu einem schlüssigen ökohydrologischen Gesamtbild mit allerdings teilweise klaren Unterschieden zwischen den Baumarten. Zusammenfassend konnte für *Alnus incana* und *Pinus pinea* ein höherer Wasserverbrauch festgestellt werden als für *Quercus suber*, der sich durch schnelleres austrocknen der Böden, sowie höhere Fließgeschwindigkeiten im Xylem zeigt.

Insbesondere für das Entwickeln von nachhaltigem Forstmanagement in zukünftigen Klimaszenarien können die hier verwendeten Messmethoden eine entscheidende Rolle spielen. So können Themen bezüglich Wassernutzung der Bäume aber auch kurzzeitig und schnell ablaufende hydrologische Prozesse in Bäumen, wie z. B. temporäre Wasserspeicherungen im Holz oder Wasserauf- und abnahme über die Rinde durch das Nutzen von hochauflösenden Tracermessungen besser verstanden werden.

Keywords: Ökohydrologie, stabile Wasserisotope, Pflanzenwasseraufnahme, *in-situ* Isotopensonden, $\delta\ ^{2}H$, $\delta\ ^{18}O$

1 Introduction

Tree transpiration plays an important role in the global terrestrial evapotranspiration (Coenders-Gerrits et al., 2014; Jasechko et al., 2013) with notable importance for catchment scale or smaller scales (Ford et al., 2007; O'Grady et al., 1999; Wang et al., 2010). However, scaling down to a single tree or plant system, ecohydrological processes related to water uptake, usage and consequently transpiration rates are not yet fully understood (Mahindawansha et al., 2018; Sprenger et al., 2019). Especially measuring root water uptake, rather than estimating it from underground plant biomass remains challenging, due to appropriate methodology (Kulmatiski and Beard, 2012; Volkmann et al., 2016b). At the same time water consumption by plants and transpiration rates are essential flows within water balance equations for soils, catchments or other properties (Brutsaert, 2014).

To answer these ecohydrological research questions, stable water isotopes tracers became more and more popular over the last decades, using natural signals like seasonal changes of isotope composition or controlled manipulated isotope signals in irrigation water (Ehleringer and Dawson, 1992; Gat and Gonfiantini, 1981; Goldsmith et al., 2012; Leibundgut, 2009; Orlowski et al., 2016b; Rothfuss and Javaux, 2017; Walker et al., 1994). Moreover, recent studies working with isotope tracers suggest a highly complex system of plant water uptake, which is in contrast to often used simplifications in soil-plant models (Allen et al., 2019; Brooks et al., 2010; Evaristo et al., 2015; Lawrence et al., 2011; Sprenger et al., 2019; Wigmosta et al., 1994, and many more).

Stable water isotope ratios ($^{2}H/^{1}H$ and $^{18}O/^{16}O$) are assumed not to be absorbed, degraded or delayed when water moves through ecosystems (Ehleringer and Dawson, 1992). Hence they are known as conservative ideal tracers which help to investigate and quantify ecohydrology processes, like plant water uptake through ecosystems.

By using stable water isotopes as tracers, it became possible to link plant water uptake to potential water sources, such as groundwater, precipitation, stream or bound soil water. This works because each water pool has its own unique stable water isotope signature due to underlying physical or chemical fractioning processes (Dubbert et al., 2019; Ehleringer and Dawson, 1992; Evaristo et al., 2015). Natural differences of stable water isotopes are detectable up to small differences and occur among other reasons due to available energy differences or different phases of water. This leads to generally lighter isotope composition in water vapor, which in the same time causes slightly enriched liquid water (Leibundgut, 2009). Thus, evaporation and transpiration both lead to a relative accumulation of heavier water isotopes in the liquid water, which can be illustrated via evaporation water lines in soils (Benettin et al., 2019; Dubbert et al., 2019) or during transpiration processes in leaves or

evaporation through the tree bark (Feakins and Sessions, 2010; Oren and Pataki, 2001; Zhao et al., 2016). Seasonality effects on the other hand are based on energy availability, showing more enriched (heavier) isotope signals for summer than for winter precipitation (Leibundgut, 2009). Both, natural isotope variation and artificial isotope tracer experiments are crucial for our today knowledge about ecohydrological plant processes with increasing importance over the last years (Rothfuss and Javaux, 2017).

By improving the experiment set-ups and measurement techniques, a more and more detailed understanding of ecohydrology processes became available. Hence, investigations of plant water usage by Ellsworth and Williams (2007) show first for erophytic and halophytic plants that their water sources and xylem water differ in stable water isotope signals. Such findings are later confirmed by many other studies, where plant water isotope signals show offsets from soil water or other potential water sources in dual isotopes plots (Brooks et al., 2010; Evaristo et al., 2015; Goldsmith et al., 2012; Hervé-Fernández et al., 2016; Sprenger et al., 2016). These studies conclude that two distinguishable water pools must be present in the soils: one water pool of mobile water without plant interaction and another water pool supplying the tree demand, which is described as bound soil water that does not contribute to stream flow or ground water recharge (Evaristo et al., 2015).

McDonnell (2014) summarizes these discoveries in the two water worlds hypothesis, describing a bound and a mobile soil water pool, distinguishable from local meteoric water lines. According to this hypothesis plants would use the bound water, which does not contribute to stream flow but is preferably taken by trees. Furthermore, other studies found that the two water pools might temporally be connected or recharged, as Allen et al. (2019) demonstrate for an experiment in Switzerland. Here xylem isotope signals in beech and oak trees show similarities with winter rains. Also Hervé-Fernández et al. (2016) found an interaction between the two water pools observed in evergreen species during the wet season in south-central Chile. On the contrary, Brooks et al. (2010) conclude in a Mediterranean climate that the small soil pores are refilled by first rainfall events after dry summer periods, during which the bound water was transpired.

However, the two water worlds hypothesis is highly discussed in the context of accuracy of the measurement methods, the assumption of no water fractioning within the plant system and our to-date knowledge about plant water uptake (Berry et al., 2017). Thus, plant water uptake from the tightly bound soil water is hard to explain with the classical view of passive hydraulic lift along the decreasing water potentials, which would suggest more likely free moving water for water uptake (Caldwell et al., 1998).

Recently, more studies are questioning the assumption that stable water isotopes travel without fractioning processes through the soil – plant – atmosphere continuum, which is a prerequisite for the two water world hypothesis (Barbeta et al., 2020; Ellsworth and Williams, 2007; Pfautsch et al., 2015; Poca et al., 2019). It has

been found out that water uptake processes in the root system can cause isotope fractioning for drought and salinity tolerant plants (Ellsworth and Sternberg, 2015; Ellsworth and Williams, 2007). This effect even increases for Acacia trees, when arbuscular mycorrhizas are present (Poca et al., 2019). Even for water transport between roots or stem tissue to xylem sapwood, deuterium fractioning processes can be present, questioning the use of stable water isotopes as ideal tracer within trees (Zhao et al., 2016). Other issues related to water travel times emerge due to disconnected water pools in trees, when water, including tracer signals, is captured temporally in tree tissues. This might happen at short temporal scales within observed phloem-xylem water exchange in Eucalyptus trees (Pfautsch et al., 2015) or through consumption and replenishing of tree internal water storages (Barbeta et al., 2020; Schepper et al., 2012). Hence, Barbeta et al. (2020) concluded that samples of xylem water hold an isotope mixture of mobile vessel water and stored vessel water, which might be subject of depletion and therefore might cause sample contamination and an offset between xylem and soil water. Influences of phloem water or temporal stored water are especially problematic for water travel time analysis in sapwood only. For longer time scales Dubbert et al. (2019) argue that isotopic offsets between soil and plant water versus groundwater can arise due to spatio-temporal dynamics instead of processes discussed in the two water world hypothesis (Berry et al., 2017; McDonnell, 2014).

It can be concluded that the method of stable water isotopes as ecohydrological tracer, as well as the outcomes from studies using these tracers, are currently highly discussed. Additionally, it should be considered that most studies focus only on one or a few plant species, thus, the huge range of species with many different water management strategies is far from being fully exploited.

Researchers using stable water isotopes rely highly on accurate measurements, which are difficult to achieve especially when the water cannot be measured direct in the compartment of interest. Traditionally, most common are destructive point measurements, for which samples need to be taken into the laboratory to extract the sample water. Among a great variety of methods, cryogenic vacuum extraction (cryo) is one of the most used and popular methods and therefore part of this study. For the isotope measurements the samples are heated up under vacuum condition to distillate the compartment water, whose steam is afterwards collected in a cold trap (Orlowski et al., 2013). The collected water then can be analysed in a mass spectrometer. However, the method was critically discussed during the most recent years, showing that soil parameters, organic contamination or measurement method and process can highly influence measurement results (Millar et al., 2018; Orlowski et al., 2016a,b). Studies comparing different laboratories supplied with identical soil samples are showing that measured results differ among laboratories although equal stable soil water isotope signals should be expected (Orlowski et al., 2018a; Walker et al., 1994). Even when extraction conditions (time, temperature, vacuum) were equal, results showed a clear variation for different laboratory setups (Orlowski et al.,

2018a). Thus, Orlowski et al. (2018a) point out that the usefulness of cryogenic extraction as a standard isotope analysing method for soils and plants should be questioned.

A frequent problem with water extracting methods is water extraction efficiency to make sure all water is measured (Araguás-Araguás et al., 1995). While cryogenic vacuum extraction performs comparably well compared to other extraction methods (e. g. mechanical squeezing, centrifugation or other techniques), the vapor equilibrium method, which recently gained attention, avoids these problems by using another measurement principal (Millar et al., 2018; Sprenger et al., 2015a). Here, samples are placed in a gas-proof closed system and equilibrated sample vapor is measured directly without water extraction (Wassenaar et al., 2008). Vapor isotope signals then can be transferred to liquid isotope signal via standards or calculations (e. g. Majoube (1971)). Compared to the cryogenic vacuum extraction, this method shows less variability in resulting isotope signatures, because laboratory work is less complicated (Millar et al., 2018; Oerter et al., 2016; Orlowski et al., 2016b; Sprenger et al., 2015a,b).

Nevertheless, both methods mentioned here, and any other method with destructive sampling, have clear disadvantages. Men power is needed to process each single sample and samples once taken cannot placed back into the experiment. Consequently, the numbers of possible samples has strong limitation, which makes high temporal resolution over longer time scales almost impossible (Kübert et al., 2020). Therefore, continuous *in-situ* measuring methods are recently introduced by different research groups to address these limitation.

In-situ measurements, so far, are based on the vapor equilibrium principals. Thus, different systems are developed, which principally consist of gas permeable tubes or probes, which allow water vapor entering a tubing system (Gaj et al., 2016; Oerter et al., 2016; Rothfuss et al., 2013; Volkmann et al., 2016b; Volkmann and Weiler, 2014). Placing measuring tubes or probes in soils or tree xylems allows to sample the pore vapor or the vapor in the xylem tissue. The sampling water vapor is transported via a carrier gas to an isotope measurement unit (cavity ring-down mass spectrometer). Hence the water vapor is in an equilibrium with the liquid water, the liquid water can be indirectly analysed similar to the vapor equilibrium method, e. g. via standards.

So far, the different developed *in-situ* methods show a wide variability of designs. For instance Gaj et al. (2016) use commercially available gas soil probes to measure stable water isotope in the soil gas. Other studies like Volkmann and Weiler (2014) or Rothfuss et al. (2013) use a more custom built approach with probes developed for only measuring stable water isotope in the water vapor. However, all methods have in common that their application in ecohydrological studies is very limited although relatively low costs and easy installing are clear advantages. Furthermore, by using a mass spectrometer as measurement unit high measurement frequencies over long time scales become available (Kübert et al., 2020; Volkmann et al., 2016a,b).

The ability of high temporal resolution measurement is crucial to better understand ecohydrological processes related to water uptake and to find solutions for the ongoing discussion about the two water world hypothesis (Berry et al., 2017). Also, analysing plant physiological processes in short time scale (e. g. temporal water storage) require isotope measuring systems. This leads to a high demand for reliable (*in-situ*) methods with high temporal resolution, which can be provided for instance through the sensor system by Volkmann and Weiler (2014).

1.1 Research Question

In-situ measurements are very infrequently used so far which consequently, means that very few experiences are available so far. This includes an application on a wider spread of species with different vessel and wood structures as well as applications in longer time scales. However, the demand of reliable stable water isotope measurements in ecohydrology and other relating research field is very high and probably will increase with future research questions.

In this study we use the *in-situ* measurement method by Volkmann and Weiler (2014) to perform a semi-controlled outdoor pot experiment with three different about 20-year-old trees (*Pinus pinea, Alnus incana, Quercus suber*). By using 20-year-old trees in large tree pots for our experiment, we are able to combine the properties of larger trees, and not seedlings, with the controlled environment of pots for the first time in *in-situ* isotope measurements. Consequently, we are able to collect information about *in-situ* isotope measurements in three more tree species. Furthermore, our, for isotope tracer experiments, relative long experiment period can help to better understand reliability of *in-situ* isotope probes by Volkmann and Weiler (2014).

By using *in-situ* isotope measurements, we can make use of the high temporal resolution and are able to avoid known issues related to destructive water extraction methods. Nevertheless, we additionally collect destructive samples during four measurement campaigns by using cryogenic vacuum extraction and vapor equilibrium method. As a result, we are able to compare and discuss measurement by different methods. Moreover, more experiences using *in-situ* methods, including comparisons of methods, are crucial for wider acceptance and eventually to replace critically discussed, but still very popular destructive methods, like cryogenic vacuum extraction.

As application, *in-situ* isotope measurements can be used to analyse tracer water uptake into the trees or tracer water travel times and velocities from the roots into and through the tree stem. However, this applications become only available through high isotope measurements in high temporal resolution and therefore, will be tested in this experiment, too. Additionally, we are able to analyse how these rarely performed analyses with *in-situ* isotope measurements are influenced by different tree species and how consistent isotope tracer measurements are with sap flow velocity measurements.

Summarising the motivation and need of investigation related to the *in-situ* method by Volkmann and Weiler (2014), this thesis addresses the following research questions:

- Can we replicate the described good performance of the *in-situ* method developed by Volkmann and Weiler (2014) under a semi controlled experiment set-up with three different trees species?
- How do these *in-situ* isotope measurements relate to destructive sampling techniques (cryogenic vacuum extraction and direct water vapor equilibration) that previously have been used for isotope measurements in trees or soils?
- Are water travel time analysis in the soil – tree continuum similar, when derived from stable water isotope tracer or sap flow velocity measurements?
- Do travel times derived from stable isotope tracer and from sap flow velocity correlate with the same explanatory variables (soil-, tree-, weather condition)?

2 Methods

2.1 Experimental set-up

The labelling experiment was carried out in a semi-controlled set-up with three approximately 20 year-old four to six meter high trees. There were two deciduous and one coniferous tree namely *Alnus incana*, *Pinus pinea* and *Quercus suber* which from here on are referred as *Alnus*, *Pinus* and *Quercus*. The location was outside in front of the Chair of Tree Physiology laboratories, University of Freiburg, in Freiburg i. Br., Germany. While precipitation on the soil was blocked by a rain-out shelter and replaced by controlled irrigation, all other conditions, such as radiation or temperature, were natural conditions. The benefit of this experiment set-up are tree sizes closer to natural forest conditions than experiments with seedling, but in the same time make use of the semi-controlled environmental conditions which would be hart to control in real outside or forest experiments.

Figure 2.1 shows a general overview of the experiment set-up including the used sensors and probes for soil-, tree- and atmospheric condition as well as isotopic signal described bellow. General location for sensors or probes were at 15 cm and 30 cm depth in the soils and at 15 cm and 150 cm height in the trees.

For the experiment the trees where planted into large pots (0.75 m x 1.3 m x 0.6 m, w x l x h), letting the root bale (0.5 m in diameter) with the previous organic-dominated soil from the tree nursery. Afterwards the pots were filled up 0.5 m with clay-silty soil (table 2.1), while the root bale surface stayed at the soil surface. To avoid water saturated soil condition at the bottom of the pots, a drainage system with collecting container was installed.

The experiment started on September 7th, 2019 and ended on November 11th, 2019 (approximately nine weeks). To minimize any influences of previous soil water on the labelling experiments, the set-up was installed up four weeks in advance to reduce the amount of water with unknown stable water isotope signal. This was done by drying out the soils as much as possible without generating to much water stress for the trees. Before the experiment set-up the trees were standing outside in the rain but trees were irrigated with 20 mm tap water three days before experiment start in order to prevent water stress damage to the trees.

2.1.1 Deuterium labelling

During the experiment two irrigation / labelling events were carried out with two differently deuterated waters shown in table 2.2. The aim was to trace the two isotope label pulses in the soil profile and in the tree xylem at several depths and heights. These data could be used to calculate travel times along the soil-plant continuum. The second labelling was conducted as a replicate.

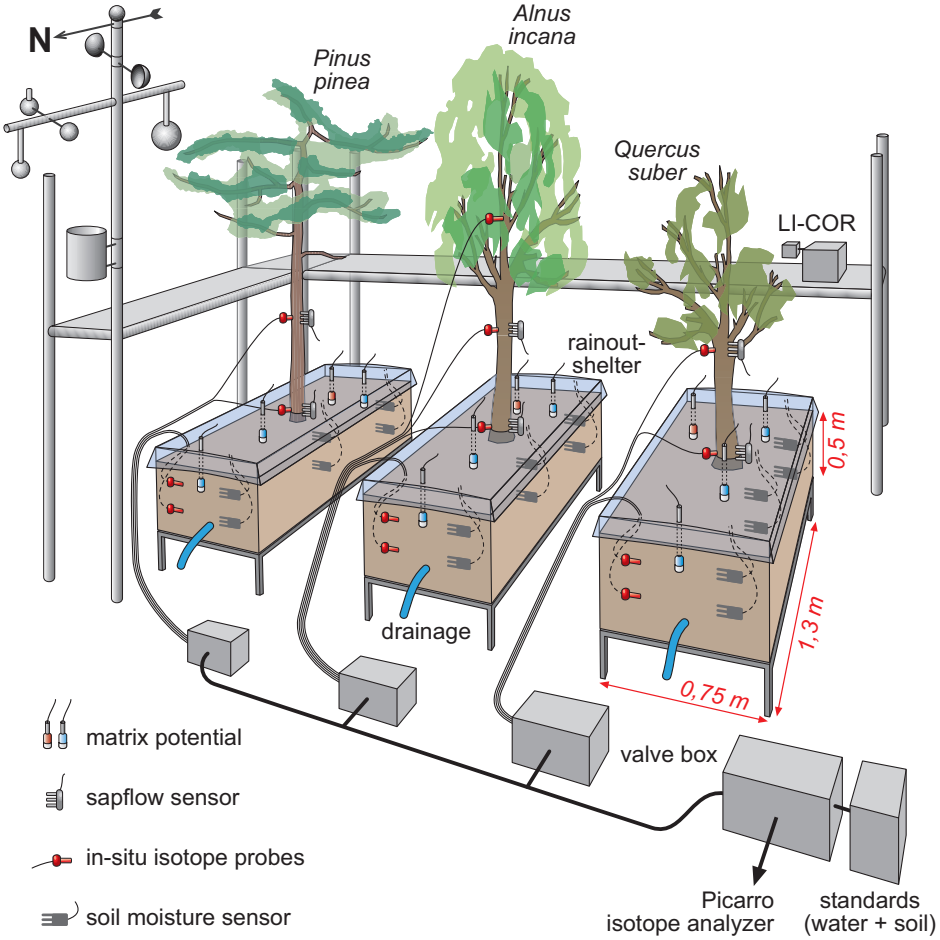

Figure 2.1: Experiment set-up including used sensors and probes as well as the valve and tube set-up for the stable water isotope probes. Trees were exposed to outdoor conditions except for natural rainfall which was to prevent unknown water input into the soil. Note that scales for tree heights or equipment are not representative.

2.2 Stable water isotopes measurement

Deuterium and the oxygen isotope ^{18}O concentrations were measured in references per thousand unit, ‰ in the so-called δ notation.

For a given isotope (here ^{18}O or ^{2}H) the δ-values are defined as

$$\delta = \left(\frac{R_{sample} - R_{reference}}{R_{reference}} \right) * 1000‰ \quad (1)$$

where R_{sample} is the ratio of the analysed isotope to the most abundant isotope for a given element in a sample (^{2}H / ^{1}H or ^{18}O / ^{16}O), and $R_{reference}$ is the ratio of Vienna Standard Mean Ocean Water (VSMOW) for the same elements and isotopes.

Table 2.1: Characteristics of the soil used for the experiment. Note that grain size distribution was analysed after removing the carbonate content with hydrochloric acid. Calcium carbonate content was relatively high and might prevent grain dispersion.

parameter		value	unit
grain size distribution	coarse sand	0.5	%
	middle sand	1.9	%
	fine sand	7.4	%
	silt	81.3	%
	clay	8.9	%
German Soil Classification (KA5)		Ut2	
carbon content	fine grained	18.5	%
pH		8.2	
max. water storage capacity*		62.5	%

* Gutachterausschuss Forstliche Analytik (2015)

Table 2.2: Applied irrigation / labelling water during the experiment. Labelling 1a and 1b are considered as one labelling /irrigation event divided into two rounds.

irrigation campaign	date and time (local time)		amount [mm]	deuterium signal $\delta\ ^{2}H_{VSMOW}$	^{18}O signal $\delta\ ^{18}O_{VSMOW}$
labelling 1a	09.17.19	21:15	20	41	-9.2
labelling 1b	09.18.19	10:30	20	41	-9.2
labelling 2	10.10.19	20:30	40	95	-9.2

Additionally, the stable water isotopes $\delta\ ^{18}O$ and$\delta\ ^{18}$ O can be related to each other by the deuterium excess (d) [‰] using the following equation derived by Froehlich et al. (2002); Merlivat and Jouzel (1979):

$$d = \delta\,^{2}H - 8.13 * \delta\,^{18}O \tag{2}$$

The deuterium excess is related to the global meteoric water line (GMWL) and can be used to investigate physical different behaviour of the stable water isotopes such as physical conditions during the formation of water vapour (Froehlich et al., 2002).

In-situ isotope monitoring

Probes for stable isotope measurements by Volkmann et al. (2016b) were installed at 15 and 30 cm depth in the soil (southern side) and at about 15 and 150 cm height in the stem at each tree pot. For *Alnus* a third stem isotope probe was installed at 270 cm height to collect data closer to the tree crown.

To install *in-situ* isotope probes in the soil we dug holes from which small horizontal holes were drilled with a screwdriver in the undisturbed silky soil. In these small holes we pushed the probes before they were covered with soil. For xylem *in-situ* isotope measurements we first removed the bark and then we drilled 3 cm deep holes with a 1 cm wood drill. The holes in the trees were deep enough to cover the micro porous tube of the isotope probes while additionally the hole with the probe was sealed towards outside influences, like the atmospheric air, with silicon.

Used *in-situ* probes measure the isotope signal within the water vapor phase, which is assumed to stay in an equilibrium with the liquid water phase as explained in the introduction. These probes were developed and tested in trees and soils by Herbstritt et al. (2012); Volkmann et al. (2016b); Volkmann and Weiler (2014).

We used *in-situ* probes with three attached gas transport lines, called diffusion dilution sampling (DDS) method (Volkmann and Weiler, 2014). Here the gas transport lines correspond as sampling, dilution and compensation (also named throughflow) line, marked with blue, red and black heat-shrink tubes. The sampling line transports the gas from the probes towards a cavity ring-down spectrometer (Picarro L1102-*i*, Picarro Inc., USA) which analyses stable water isotopes and humidity in quasi-continuous time steps. The compensation line is necessary to maintain the pressure equilibrium with the surroundings because otherwise an under-pressure would constantly generate a flow of water vapor towards the probes. Likewise, dilution of vapor sample with dry air is useful to avoid condensation in the gas tubes which can occur when air temperature is lower than the temperature in the tree xylem.

The probes itself consists of three parts connected via sealed threads. At the probe head enters the vapor the probe through a rigid hydrophobic microporous polyethylene probing tube (outer diameter: 10 mm; length: 30 mm; Porex Technologies, Germany). Here the compensation line ends to maintain the pressure equilibrium which was assumed not to affect the vapor exchange. Dilution and sampling line end in a openly connected mixing chamber (manufactured from PVDF, Fischer Plastics) below the porous probe head. On the bottom the mixing chamber is closed and connected to a rigid insertion for protection and installation purpose. More detailed information about the isotope probes can be found in Volkmann and Weiler (2014).

As dilution and carrier gas we used synthetic air from 10 l gas bottles which, in terms of carrier gas for isotope sampling performs similarly to nitrogen used by Volkmann and Weiler (2014) (Gralher et al., 2016). The pressure of synthetic air was reduced to approximately 4 bar by using a pressure regulator with gauge before split up into dilution line and compensation line. Flow of dilution was regulated with a digital flow controller (Digitaler Strömungsregler Serie 358, Kat.Nr. 35828; Analyt-MTC GmbH, Germany; 0 - 200 mL/ min, uncertainty +/- 1%) to 35 mL/ min during flushing period and 10 mL/ min during measurement period. Compensation flow was regulated to 25 mL/ min only during measurement period using a digital flow controller (Digitaler Massenflussregler GFC 171, Kat.Nr. 35362; Analyt-MTC

GmbH, Germany; 0 - 50 mL/ min, uncertainty +/- 1%). Both flow controllers were controlled via an analog voltage signal between 0 V (no flow) and 5 V (maximal flow) by a self-built electric circuit of an Arduino-Uno PWM Signal (Arduino-Uno, `www.arduino.cc`). To produce a smooth voltage signal between 0 V and 4.5 V, two capacitors were used. Finally the Arduino-Uno was connected via USB to the Picarro computer (Picarro L1102-*i*, Picarro Inc., USA) and managed by a Python-GUI, which controlled the entire measurement and flashing routine.

Before each measurement the probes and tubing were flushed with synthetic air to remove the pre-existing air from the system. Here, flushing period lasted for maximal 30 min per measurement probe and was followed by a maximum 15 min long measuring period per probe. If stable measurement conditions were established in terms of humidity and isotope signal the controlling program changed to the measuring period or the next isotope probe before the maximum time reached. Typically the flushing period was visible as a drying period (Picarro's H_2O concentration measurement) while the measuring period was wetter than the end of the flushing period, however, less wet than at the start of the flushing period. In addition to cleaning the probes, the flushing periods avoid contamination effects caused by previous used isotope probes. If measurements failed because of too high humidity in the probes or in the tubing system, the system and sensors where flushed with dry air for longer time periods as well as flow rates were temporarily increased.

A complex gas line circuit (figure 2.1) with valve boxes made it possible to connect each individual isotope probe (trees, soil and standards) with the compensation and dilution input lines on the one side and with a cavity ringdown spectrometer (Picarro L1102-*i*, Picarro Inc., USA) via the sampling line on the other side. The self-built valve boxes were controlled by micro controllers and consist of $8 * 3$ ($*3$ for each gas line) valves (EC-2M-12, Clippard, USA) for the three tree pots. The third xylem sensor for *Alnus* (270 cm height) and the standards were connected via a $6 * 3$ valves box (E10M-04, Clippard, Ohio, USA) to the Picarro.

The tree valve boxes were installed in series connection with self 3D printed and sealed with epoxy resin adhesive (2-K-Epoxidkleber, UHU GmbH & Co. KG, Germany) intersections connectors. This meant that tubes added up from approximately 9 m (*Quercus*) to 12 m (*Alnus*) in lengths because in contrast to the trees measurement equipment was stored in a sheltered location. For gas lines we used Teflon (FEP) tubes (KAP 100.968, Techlab, Germany) with 1/16" diameter which were placed in one bigger plastic tube (diameter: 1 cm) for protection purpose.

To transfer vapor measurements by the isotope probes into liquid values, we used three soil standards and three water standards described in table 2.3. The calculations for using the standards are explained in section 2.5.1 in data processing. By using water and soil standards we tried to compare both types of standards however, this was not possible in the end.

Table 2.3: Soil and water standards for *in-situ* stable water isotope measurements.

name	type	δ ^{2}H in ‰	δ ^{18}O in ‰
stdSL	soil low	-82	-11.1
stdSM	soil middle	-32	-8.2
stdSH	soil high	20	-5.0
stdWL	water low	-82	-11.1
stdWM	water middle	-32	-8.2
stdWH	water high	20	-5.0

The standards were stored in airtight containers of polyvinyl chloride (PVC-U) drainage pipes (KGU 125, Ostendorf KG, Germany; length: 14 cm, diameter: 12.5 cm), available in hardware stores, with cuff sleeves at both ends. The ends were closed with fitting seals (Ostendorf KG, Germany) and in the top cap a sealed opening for cables was installed. For the soil standards we used 1200 g oven dried (200 °C for 24 h, cooled down in desiccator) sifted silty soil from the tree pots with 300 ml added isotopic water solution. Consequently, for water standards we only were 150 ml isotopic water solution. All standard water solutions were mixed first before they were filled in the containers.

Finally, the same stable isotope probes as used for xylem or soil measurements were placed in the soil for soil standard or in a hanging position above the water level for water standards. Additionally, each standard was equipped with a soil moisture sensor (5TE, Labcell Ltd, USA) pushed in the soil or placed in the water, which was then connected to a data logger (EM50, Decagon Devices Inc., USA). All standards were placed in a styrofoam box to avoid temperature and evaporation effects.

Beside the *in-situ* measurements, all standards were also tested with destructive measuring methods as described below.

Destructive isotope measurements

We used two methods of destructive measurement methods (cryogenic vacuum extraction and direct water equilibrium methods) were used at four different measurement campaigns pointed out in table 2.4. In general, twigs were collected in two different heights in the tree crones and placed with removed bark in the sample containers, while for soil samples one soil core per method was divided into two depths (0-25 cm and 25-50 cm) corresponding to 15 cm and 30 cm depth. Consequently, isotope measurements by destructive methods can be compared with *in-situ* isotope measurements when twigs samples are used as equivalent to xylem measurements.

Cryogenic vacuum extraction ("cryo"):

Water extraction via vacuum followed by isotope measurements of extraction water is a common method used to analyse stable water isotopes of soil or plant

Table 2.4: Dates for destructive sampling campaigns of "cryo" = cryogenic vacuum extraction and "bag method" = direct water vapor equilibration. Material was collected around noon and directly stored in sealed containers.

Date	Method	Type
09.16.2019	soil & xylem	bag method & cryo
10.02.2019	soil & xylem	bag method
10.28.2019	xylem	bag method
11.14.2019	soil & xylem	bag method & cryo

material (for example Allison and Hughes (1983); Araguás-Araguás et al. (1995); Orlowski et al. (2016a, 2013); Walker et al. (1994) and many more). We used a custom built cryogenic vacuum line set up in the laboratory of the Chair of Tree Physiology, University Freiburg, to extract xylem and soil water (see Dubbert et al. (2014, 2017) for further information). Here samples were heated in 12 ml glass exetainer (LABCO, United Kingdom) for 90 min in a 95 °C warm water bath under a vacuum of at least 0.08 mbar. Extracted vapor was trapped in glass tubes tucked in liquid N_2. Afterwards, samples were defrosted and filtered for measuring δ isotope values with a liquid ring sprectrometer (Picarro L2130-*i*, Picarro Inc., USA).

Direct water vapor equilibration ("bag method"):

Direct water vapor equilibration is based on an isotopic equilibrium, which in a closed system (e. g. metallized sampling bags) establishes within a few days between liquid and the vapor phase (Sprenger et al., 2015a,b; Wassenaar et al., 2008). Consequently, the method measures the isotope ratio of the water vapor which corresponds to the liquid (pore) water. The advantage is that water does not need to be extracted and the water vapor can be analysed with a laser spectroscopy. The method was first developed by Wassenaar et al. (2008) and subsequently used and improved within many other studies (Hendry et al., 2015; Hendry and Wassenaar, 2009; Stumpp and Hendry, 2012, and others).

For stable water istope measurements, at least 30 g material was collected and directly filled into metallized sampling bags of tri-ply, adhesive laminated sheets including one 12 mm layer of aluminium foil (1 L volume, Item no. CB400-420 BRZ, Weber Packaging, `http://www.weber-packaging.de`). In the laboratory the sample bags were filled up with dry air (pressure about 1 bar) before heat-sealed. Afterwards tree samples were allowed to equilibrate one day, while the soil samples equilibrated two days in the laboratory (20 °C) before the measurements. The vapor in the bags was measured with a cavity ring-down spectrometer (Picarro L2120-*i*, Picarro, USA) with a needle through a previously added silicon drop for sealing reason. Once isotope and humidity measurements were stabilized, average values of $\delta\ ^{2}H$ and $\delta\ ^{18}O$ over 90 s were as data point.

To transfer vapor into liquid isotope values three standards of 10 ml each (FSM: δ^2H = -126.2, δ^{18}O = -16.7; tap water: δ^2H = -65.88, δ^{18}O = -9.55; Baltic Sea: δ^2H = -2.61, δ^{18}O = -0.41) were handled like the samples and measured before and after the samples.

2.3 Atmospheric and soil condition

For atmospheric measurements the data provided by the German weather service (Deutscher Wetterdienst) station Freiburg i. Br., Germany (station id: 1443, N: 48.0232, E: 7.8343, elevation 237 m, temporal resolution: 10 min), less than 1 km away from the experiment site, was used. We used data of air temperature (T_a) in 2 m height, total solar radiation (TSI) and relative humidity (RH) and calculated from these data hourly vapor pressure deficit (VPD) values using the Teten formula, which is commonly used by the Food and Agriculture Organization of the UN (Allen et al., 2004; Junzeng et al., 2012).

Soil moisture and soil temperature were monitored with 5TE sensors (Labcell Ltd, USA) at two depths (15 and 30 cm) at both sides of the pots in the silty soil (north and south) plus in the root bale (southern side). 5TE sensors were pushed into undisturbed soil to measure volumetric water content with a VWC resolution of 0.08 % to 50 % VWC (Decagon Devices, 2007).

Soil metric potential was recorded as hPa and transformed into pF values using matrix potential sensor (MPS, Decagon Devices, USA). Three MPS sensors per tree pots were placed at 15 cm depth close to the 5TE sensors (south, north and root bale).

Sensors installed in the root bale were installed before filling up the tree pots with soil, while the other sensors were installed from small dug holes at each side of the tree pots. All sensors installed in the root bale were connected to a data logger (CR1000, Campbell Scientific Inc., USA), whereas the other sensors were connected to four smaller data loggers (EM50, Decagon Devices Inc., USA). Over the course of the experiment all data was stored in 10 min intervals.

2.4 Tree conditions

2.4.1 Sap flow velocitiy

Heat pulse sap flow sensors (SF3 3-needle HPV Sensor, East 30 Sensors, USA) were installed on the north-facing sides of the stems at 15 cm and 150 cm height. The tree bark was removed beforehand and sensors were installed in drilled holes using a drilling guide for correct distances in between needles. Afterwards, the sensors were hold in place with tree glue and covered with reflective isolating foil to prevent air temperature and solar radiation influences.

The sap flow sensors measured the response of a heat pulse initiated by the middle needle at the both outer needles. The change of temperature and runtime of the heat pulse signal then can be transformed into a sap flow velocity (V_{sap}) using the concept of Cohen et al. (1981). Here used sensors had three measuring positions at each needle at 5, 18 and 30 mm depth, referred as outer, middle and inner position. Sap flow velocities were stored in a 10 min interval on a data logger (CR1000, Campbell Scientific Inc., USA).

To transfer the heat pulse signal into velocity we used equation (3) by Hassler et al. (2018), who derived their equation from Campbell et al. (1991):

$$V_{\mathrm{sap}} = \frac{2k}{C_w(r_{\mathrm{u}} + r_{\mathrm{d}})} \ln\left(\frac{\Delta T_{\mathrm{u}}}{\Delta T_{\mathrm{d}}}\right) \tag{3}$$

where k is the thermal conductivity of the sapwood, set to $0.5\,\mathrm{W\,m^{-1}\,K^{-1}}$, C_w is the specific heat capacity of water in $\mathrm{J\,m^{-3}\,K^{-1}}$, r is the distance between heating (middle) and measuring (outer) needles in m (here 6 mm) and ΔT is the temperature difference before heating and 60 s after the heat pulse in K. Indices d and u stand for downwards and upwards compared to the heated needle in the middle.

Sap flow velocity was additionally corrected for wounding of the xylem tissue and installation effects using equation (4) according to Burgess et al. (2001):

$$V_{\mathrm{c}} = b\,V_{\mathrm{sap}} + c\,V_{\mathrm{sap}}^2 + d\,V_{\mathrm{sap}}^3 \tag{4}$$

where V_{c} ($\mathrm{m\,s^{-1}}$) is the corrected V_{sap} and b, c and d are the correction coefficients. Since we used the same equipment as the one chosen by Hassler et al. (2018), the same correction coefficients were applied, meaning $b = 1.8558$, $c = -0.0018\,\mathrm{s\,m^{-1}}$ and $d = 0.0003\,\mathrm{s^2\,m^{-2}}$ (Burgess et al., 2001; Hassler et al., 2018).

To remove outliers, we applied a rolling median and mean after each other over 30 min on the calculated sap flow velocities. Furthermore, we used only the measurements at the outer sensors of the measurement needles since we mainly used sap flow velocity data to compare it with tracer travel times. Difficulties with the heat ratio method, relating underestimated peak velocities or not ideally installed sensors are known and reported by various authors (Fuchs et al., 2017; Hassler et al., 2018; Vandegehuchte and Steppe, 2013). Here general offsets were corrected by shifting values in a way that nightly sap flow velocity was around zero. This approach is similar to Pfautsch et al. (2010), who are using dark periods during 24 hour rain fall events as zero sap flow velocity point. However, this method requires longer time periods and does not correct data shifts in short temporal resolution, which is why we used a different approach.

2.4.2 Photosynthesis and conductance

A portable photosynthesis system (LI-6400XT, LI-COR Biosciences Inc., USA) was used to measure maximum photosynthesis rates and conductance of water vapor for

Table 2.5: Modified chamber settings for the LI-COR LI-6400XT which are applied additionally to the general set-up suggested by LI-COR Inc (2012) and Evans and Santiago (2014).

Flow Rate	=	$500\,\mu mol\,s^{-1}$
CO_2 Reference	target =	$450\,\mu mol\,mol^{-1}$
Temperature Control	constant block temperature =	$20\,°C$
Lamp Control	PAR =	$1500\,\mu mol\,m^{-2}\,s^{-1}$
Relative Humidity	approximately	65 %

the tree leaves. We followed mainly the protocols by LI-COR Inc (2012) and Evans and Santiago (2014) with modified chamber settings according to table 2.5.

Photosynthesis and transpiration measurements were collected on days without rain once per day, around noon. One photosynthesis and transpiration value consisted of the average values measured at four leafs per tree at different heights (bottom to top of the crown) and sun exposition. Furthermore, one leaf measurement was repeated four times and averaged once LI-COR chamber conditions were stabilized.

2.5 Data processing

2.5.1 *In-situ* isotope measurement data

To process the measured isotope data, first data points with obvious errors or technical failures were eliminated following the criteria in table 2.6. In general, the median of the last 4 min of the measuring period was used as data point for δ isotope values.

Table 2.6: Criteria for elimination of outlieres in isotope data points by the ring down spectrometer. (Data fulfilling the criteria was eliminated.)

testing parameter	criteria
valve switch failure	total valve open time $< 280\,s$ or $> 4000\,s$
flushing	per sensor activation (flushing and measuring period): less than 10 H_2O values $< 0.8 * \overline{x}$ of first and last 10 H_2O values
impossible data	δ^2H lower than tap water ($\delta^2H = 94$)
humidity	H_2O (humidity, ppm) > 3500 & < 35000

Correction regarding humidity was performed according to Brand et al. (2009), who show that humidity has a significant impact on the isotope measurements. For $\delta\ ^{18}O$ values they found linear deviation, while for $\delta\ ^{2}H$ the deviation is linear above 12 500 ppm H_2O and becomes increasingly non-linear for humidities below 10 000 ppm (Brand et al., 2009).

We assumed for humidity correction a linear deviation for both stable water isotopes and corrected $\delta\ ^{2}H$ and $\delta\ ^{18}O$ separately for standard, soil and xylem probe measurements with equation (5) to 12 000 ppm because median and mean values for all measurements were slightly above 12 000 ppm.

$$y_c = ((12000 - x) * a) + y \tag{5}$$

Here y is the uncorrected $\delta\ ^{2}H$ or $\delta\ ^{18}O$ value and y_c is the corrected $\delta\ _{2}H$ or $\delta\ ^{18}O$ value of y. The slope of the linear equation (a) was calculated separately for the isotopes using all uncorrected data points and was applied on the uncorrected data points y with the humidity x [ppm].

To transform vapor isotopes values in liquid isotopes values, we used the six standards of which the stable isotope value of the water was known and additionally measured with destructive methods and a ring-down spectrometer for water (Picarro L2130-*i*, Picarro Inc, USA). For each tree or soil probe measurement x_i the six standard measurements before and after x_i in a time perspective were selected and a linear model for vapor against liquid values was calculated. Finally, the resulting linear equation was used to determined the liquid isotope δ value for the measured vapor isotope signal x_i.

2.5.2 Outlier handling

Generally, outliers of measured tree and soil conditions (soil moisture, water potential) were very unlikely only sap flow velocity needed correction, but those data points were clearly identified due to impossible values.

To identify outliers for the isotope data, a cluster approach per each valve and tree was used. We used the hierarchical agglomerative clustering method combined with single linkage method, which merges always the most similar clusters related to the nearest neighbours starting from each single observation (Almeida et al., 2007; Hawkins, 1980). Similarity, or in other words distance, was calculated by Euclidean Distance (equation (7)) using a data set including corrected $\delta\ ^{2}H$ and $\delta\ ^{18}O$ data plus a time step and label period indicator at once. Euclidean Distance is described by:

$$\mathrm{dist}(x,\, y) = \sqrt{\sum_{i=1}^{n}(x_i - y_i)^2} \tag{6}$$

where x and y are two data points. Because deuterium was used as first cluster dimension the outlier reduction was stronger for deuterium than for ^{18}O measurements, which was used as second dimension. The cluster tree was reduced to $n = a/10$ (rounded) clusters, with a being the number of available data points. Finally, clusters with less than five data points were identified as outliers and, after visual examination, deleted from the data.

All data processing and statistics were carried out in R (version 3.6.1, R Core Team, 2019), using RStudio (version 1.2.5001, RStudio Inc, 2019).

2.6 Data analysis

2.6.1 Similarity of isotope signals

To detect how different the isotope probes responded after a labelling event, the root mean square difference (RMSD) between each isotope probe time series was calculated with the following equation:

$$\mathrm{RMSD} = \sqrt{\frac{1}{n}\sum_{i=1}^{n}(x_i - y_i)^2} \tag{7}$$

where x_i and y_i are daily median values for two sensor time series x and y with n numbers of observations. Days without a value for x or y were excluded from the analysis.

Other known methods for differentiation of time series including significance levels, such as autoregressive moving average (ARIMA) or Granger causality test (Granger, 1969), were tried out without promising results. Although, these tests can be used on very different datasets, originally there were developed for other purposes like economics. Furthermore, both tests have difficulties with handling inconsistent time steps.

2.6.2 Isotope travel time analyses and tracer travel velocity

To analyse the tracer responses after a labelling event in the different isotope probes, sufficient data points, especially during the times with significant signal changes, are needed. As this was not the case, analysis based on functions like Gompertz function (Laird, 1964) were not possible. Instead we used a descriptive approach and like that looked at the isotope responses after the labelling events by hand.

Consequently, we use tracer travel times which is the time that the tracer needs to travel between two measurements probes or from tracer application to the measurement probes. Furthermore, we define tracer travel velocity by dividing the distance travelled by the tracer (e. g. between two measurement points) through tracer travel time needed for this specific distance.

2.6.3 Dependencies and similarities between different parameters

In order to determine how tree activity, represented by sap flow velocity, is influenced by other parameters, we used a general linear model (GLM). Hence, sap flow velocity was used as response variable as well as soil conditions and weather conditions,

represented by VPD, were used as independent variables. Since irrigation takes place only during a single time step, we were not able to include it as an independent variable, but we assumed that water input would be represented by soil condition. Furthermore, all soil moisture sensors (south, north, root bale) at each depth were averaged. Metric potential was let out because it contained similar information as soil moisture but with less replications (sensors) available. This is shown by high correlations between soil moisture and metric potential. To eliminate effects caused by daily variation, furthermore, only the three hours with the highest averaged sap flow velocity values were used (*Pinus*: 12 until 15 o'clock, *Alnus*: 11 until 14 o'clock, *Quercus*: sensor failure).

Hence, the GLM was applied with the following parameters allowing interaction between each independent variable, represented by a star ($*$):

$$\begin{aligned} SapFlowVelocity \quad \sim \quad & VPD * SoilMoisture\,15cm * SoilMoisture\,30cm \\ & * SoilMoisture\,15cm\ (root\ bale) \\ & * SoilMoisture\,30cm\ (root\ bale) \end{aligned}$$

The GLM was calculated separately for each tree and each measurement height of sap flow velocity (25 cm and 150 cm) and label event (data between first and second labelling event, and data after second labelling event). Here normal distribution was used and independent variables were tested for correlations causing variance inflation (Dormann et al., 2012). Furthermore, independent variables interactions for the GLM-model were tested for significance (p-value < 0.05) using ANOVA and eliminated from the model when allowed by the marginality theorem. Additionally, we followed the concept of Dormann (2013, p. 153ff) for model diagnostics: checking on dispersion, residual- and outlier analysis.

Dependencies between *in-situ* stable water isotope measurements and sap flow velocities, soil moistures and VPD were tested for each isotope probe using the robust non-parametric Kendall rank correlation (Kendall, 1938).

3 Results

The result section follows mainly the research questions defined earlier however, general measurements are included as well for better background understanding. First tree-, soil and atmospheric conditions are presented since these information can be fundamental for the tracer behaviour. This is followed by the dependency analysis for sap flow velocity. Finally, results regarding the *in-situ* stable water isotopes measurements are shown and compared with commonly used destructive measurement methods. This section will close by following the third research question, comparing water travel times derived from sap flow velocity sensors and stable water isotope probes and its influencing parameters.

3.1 Soil, tree and atmospheric conditions during the experiment

Since the isotope tracer experiment is set up in trees under partly environmental influenced conditions it is crucial to know soil, tree and atmospheric properties first to understand results of isotope measurements. Thus, partly here presented results are clearly due to the semi-controlled experiment set-up. Hence, some parameters are clearly influence by natural condition, like radiation, while other parameters, like soil moisture and soil metric potential, respond evidently to the controlled part in the experiment. Thus, the irrigation / label events cause a sudden increase of VWC by at least + 10 % but the rain shelters on the other hand evoke dry periods, during which soil metric potential even exceeded the permanent wilting point (PWP) of pF-value 4.2 (figure 3.1).

However, soil moisture show strong differences between each sensor within one tree pot with highest differences for *Quercus* (range of average VWC values: 12.2 % – 32.4 %), while soil moisture measurements within *Pinus* (9.6 % – 24.5 %) and *Alnus* (13.0 % – 18.5 %) are clearly more similar (figure 3.1). Over all, median soil moisture values are highest for *Quercus* (VWC = 20.8 %) and notable lower for *Pinus* (VWC = 11.7 %) and *Alnus* (14.2 %). This is consistent with results from soil metric potential with lowest median pF values for *Quercus* compared to the other trees (pF values: *Alnus* = 3.2, *Pinus* = 2.4, *Quercus*: 2.1, see figure 3.3 and figure 3.1). Hence, these results suggest that water consumption was lower in the soil of the *Quercus* tree pot in comparison to the other tree pots. Additionally, conditions drier than than the PWP do occur in *Alnus* and *Pinus* soils but not in the *Quercus* soil pot.

Due to the experiment set up, transpiration should be the only water outflow allowed from the soils, since the installed drainage system did no become active unused. Therefore water loss in the soils should be also reflected by root water uptake and tree conditions.

Furthermore, soil conditions capture different responses for water potential and soil moisture outside and inside the root bales. Thus, for drying periods sensors in the root bales are showing mostly higher soil moisture plus higher pF values than

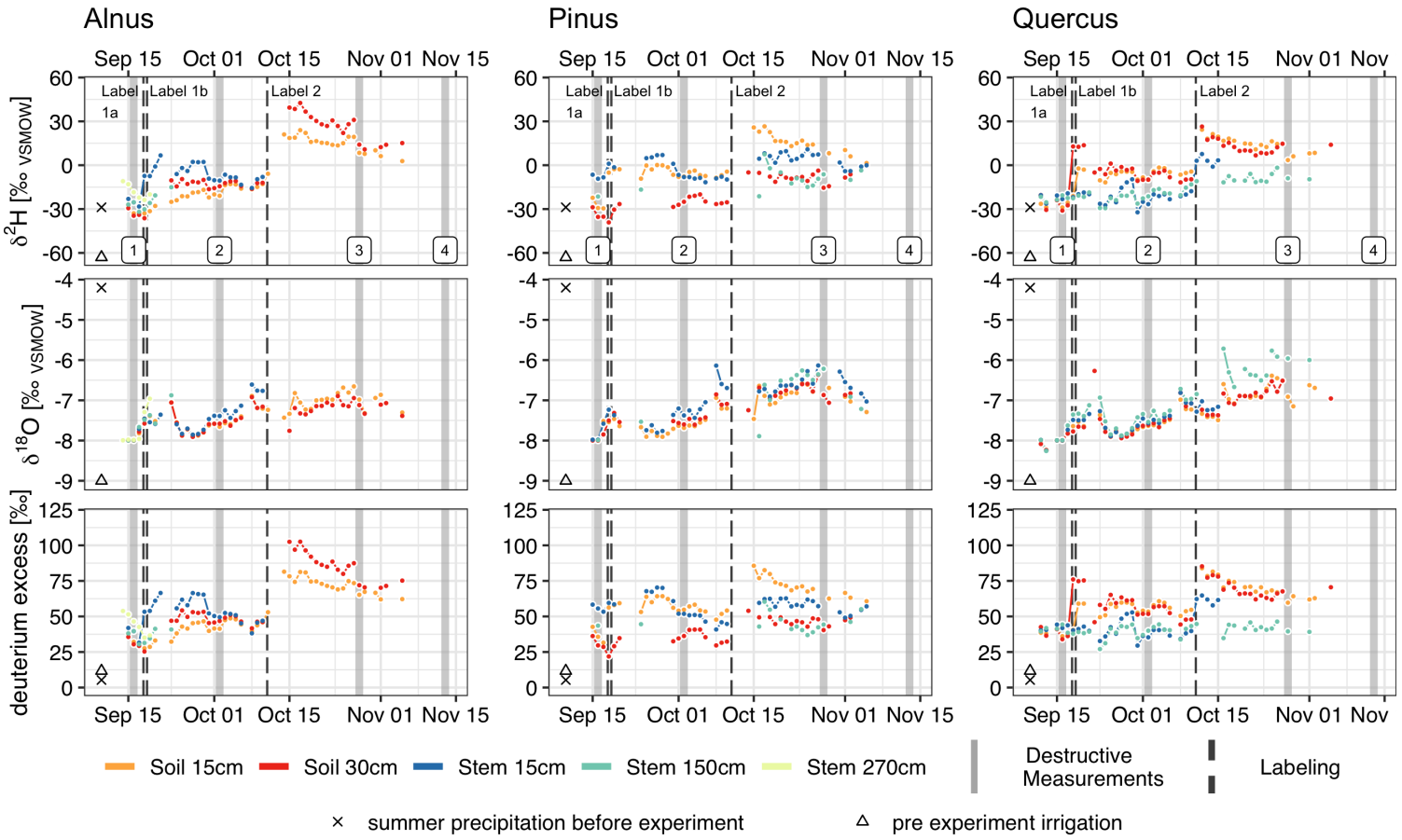

Figure 3.1: Daily median stable water isotope measurements with *in-situ* probes in xylem and soils for the three tree pots *Alnus incana*, *Pinus pinea* and *Quercus suber*. Deuterium and ^{18}O are shown in δ notation while deuterium excess bases on the following equation: $\mathrm{d} = \delta\,^{2}\mathrm{H} - 8.13 * \delta\,^{18}\mathrm{O}$. For reference, plots include destructive measurement campaigns and labelling dates as well as summer precipitation and pre event irrigation isotope signal. The connecting lines are interrupted in case of longer time periods than 24 hours in between two measurements.

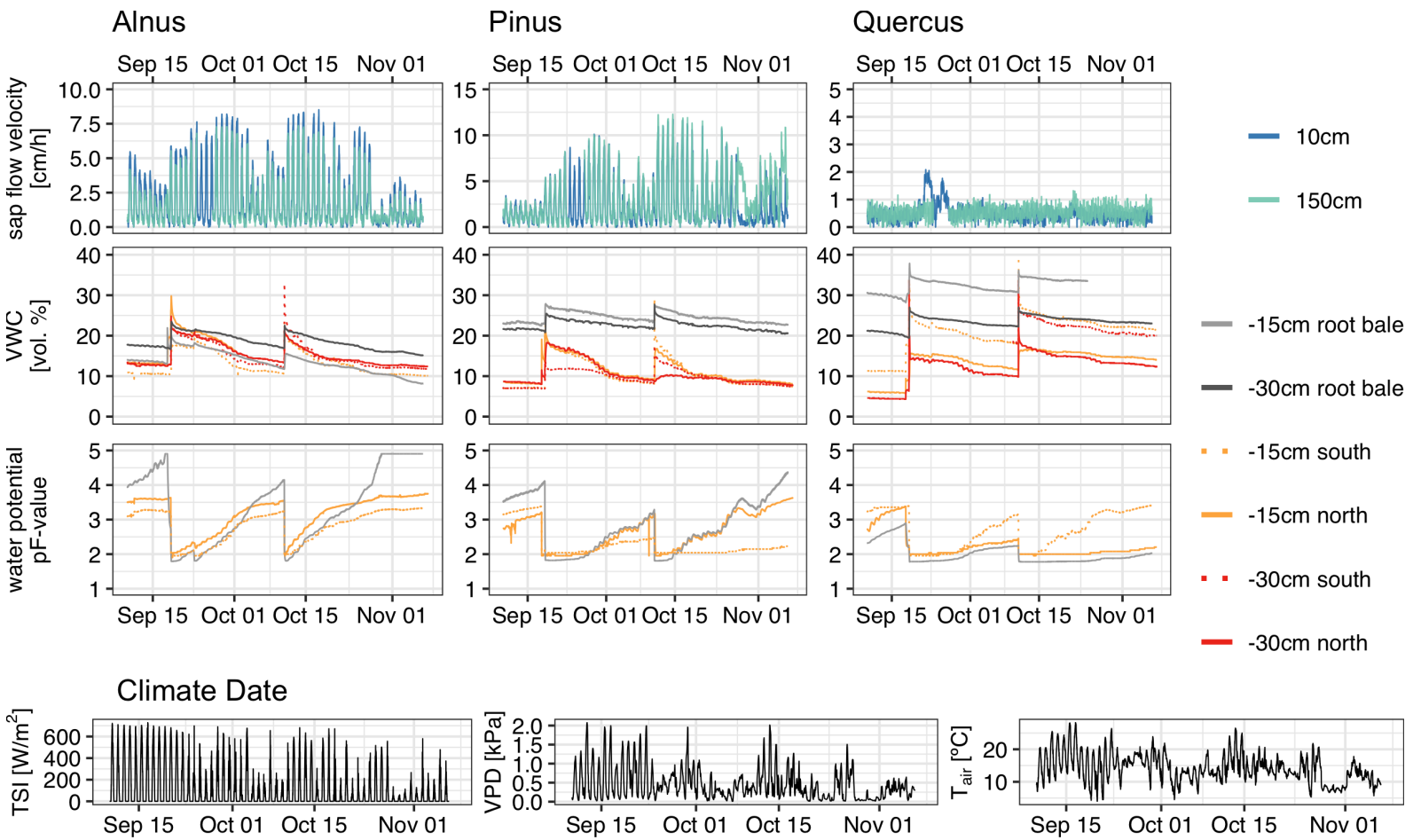

Figure 3.1: Soil-, tree- and atmospheric conditions over the course of the experiment in 10 minute temporal resolution. Soil condition and sap flow velocity is grouped into the three tree pots *Alnus incana*, *Pinus pinea* and *Quercus suber*. Climate data is provided by the German weather service station Freiburg i. Br., Germany, less than 1 km away. Sap flow velocity measurements for *Quercus suber* are influenced by sensor failures.

sensors placed in the silty soil (figure 3.1). Different soil types and water retention capacity (Blume et al., 2010, p. 229) or higher water uptake due to higher root density are possible explanations (figure 3.2 and figure A.3).

When comparing water consumption based on soil moisture with sap flow velocity, similar trends can be observed. Regarding the tree activity, *Pinus* reaches the highest sap flow velocities (max 12 cm h^{-1}) closely followed by *Alnus* with slightly lower maximum sap flow velocities (9 cm h^{-1}), whereas *Quercus*' sap flow velocity was clearly lowest for all three trees (figure A.4, figure 3.4). Furthermore, measured daily variations show that highest sap flow velocities are all around noon, with *Pinus* being one hour later than *Alnus* (figure 3.1, figure A.4, figure 3.4). Differences between the two heights are mostly visible during night, when variance in 150 cm is clearly higher than for 15 cm.

From another experiment's experiences (unpublished) we know about difficulties related to sap flow velocity measurements in *Quercus suber* trees. Hence, the very low sap flow velocities for *Quercus* might be strongly influenced by sensor failure and defensive reactions by the tree and therefore the sensor was excluded form further analysis.

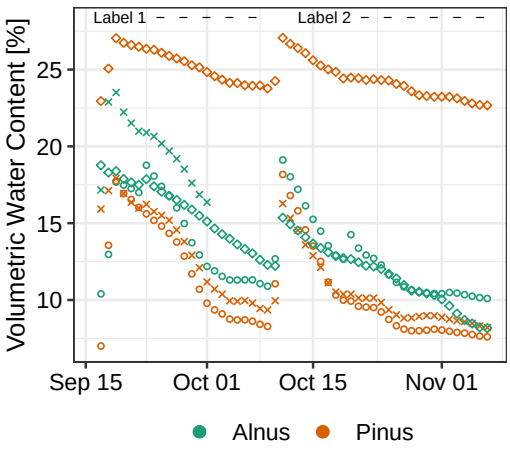

Figure 3.2: Daily mean soil moisture (VWC) of root bale (◇) northern (○) and southern (×) soil position in the tree boxes at 15 cm depth.

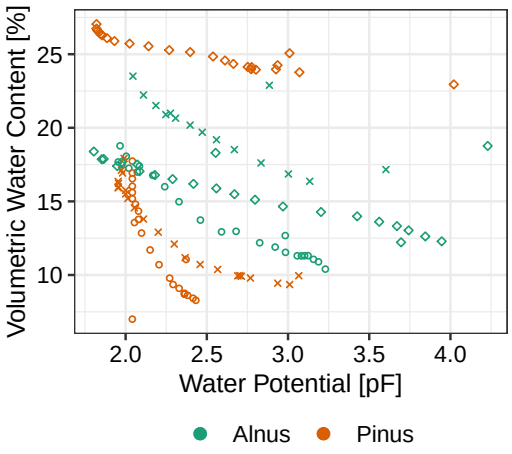

Figure 3.3: Correlation between soil moisture (VWC) and soil metric water potential (pF-value) of root bale (◇) northern (○) and southern (×) soil position in the tree boxes at 15 cm depth during the first labelling. Data points are daily mean values. See figure A.5 in the appendix for the second labelling event.

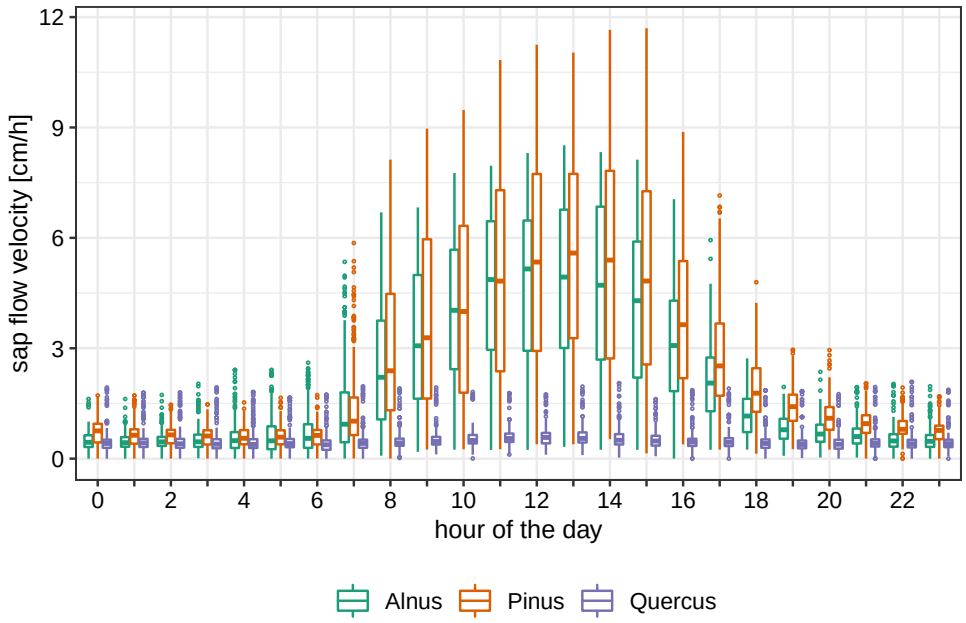

Figure 3.4: Sap flow velocities at 15 cm height for *Alnus incana*, *Pinus pinea* and *Quercus suber* grouped in hour of the day via boxplots. Due to the many measurements more outliers (dots) can occur. However, sap flow velocity for *Quercus suber* is influenced by sensor failure and therefore excluded from further analysis. (See figure A.4 in the appendix for sap flow velocities at 150 cm height.)

Measurement for maximum photosynthesis and transpiration show similar results for *Alnus* and *Quercus* which can be an indication for a healthy tree activity (figure A.1 and figure A.2). However, since the *Quercus* had very few leaves compared with the *Alnus* the complete tree transpiration is very different. Consequently much lower transpiration volumes can be expected for *Quercus* although maximum transpiration rates for single leave measurements are similar between both trees.

Additionally, the LI-COR system was modified to analyse the stable water isotopes in the transpiration water vapor. However, this set-up did work so far due to leakage and problems related to flow rates.

3.2 Influence of atmospheric conditions on sap flow velocities

To analyse the influence of independent atmospheric and soil conditions on sap flow velocities we used a GLM approach. However, to increase accuracy of the GLMs, a pre analysis of independent variables was done aiming at reducing the independent variables. Thus, high correlations between the two independent variables soil moisture and soil metric water potential are found (Kendall's $\tau < -0.88$, figure 3.3). Furthermore, by using agglomerative cluster analysis per tree and label event, two

clear differential clusters (spearman ρ^2-value > 0.5) can be seen for the whole analysis (Dormann (2013, p. 280ff); `varclus(..., similarity = "sperman")` function in the `R`-package `Hmisc`, figure A.7 to figure A.10) . The two clusters suggested are VPD, representing atmospheric condition, and a group with all soil moistures sensors (figure A.7 to figure A.10). Since the tree root growths had to start from the root bales only, we did further variable reduction, using only soil moisture probes in the root bale (15 cm and 30 cm) as independent variable beside of VPD. Correlation analyses show that soil moisture in the root bale differs only slightly from other soil moistures (figure 3.1), while trends are highly similar (Kendall's $\tau > 0.78$, figure A.6 in the appendix). When we took out the soil sensors after the experiment we were able to confirm limited root growth with high concentration to the original root bale.

Using a GLM with allowed interactions between independent variables, we generally see a positive feedback by independent variables on sap flow velocity, whenever the GLM could be reduced to a maximum of four variables. For variable reduction, including interacting variables, we applied an ANOVA on the GLM output. In detail, higher VPD, soil moisture 15 cm, soil moisture 30 cm or combining interaction are causing higher sap flow velocities for both analysed periods (table A.1 to table A.4 in the appendix). In the same models VPD and its interaction with other independent variables are always highly significant (p-values $\ll 0.05$), whereas the significance levels for other independent variables are highly variable. Generally, the differences between the two soil moistures probes are difficult to detect by looking at the models (table A.1 – table A.4) and therefore confirm findings via the cluster analysis (figure A.7 – figure A.10).

Adjusted R^2 values for successful simplified GLM models are all higher than 0.6 suggesting a relative good fit for the models (e. g. table A.1). Here, also residual plots do not show critical patterns in terms of systematic errors. However, if model simplification is less successful, significances for VPD as independent variable decreases (p-values < 0.05 instead of $\ll 0.05$) while interacting variables with VPD become more important (e. g. table A.2).

Next to GLM calculations a visual analysis shows decreasing sap flow velocity for *Alnus*, when water stress is too high (exceeding PWP) over longer periods (after October 10$^{\text{th}}$, seefigure 3.1). Here, maximum sap flow velocities are first comparably low between October 10$^{\text{th}}$ and November 1$^{\text{st}}$ for *Alnus* and *Pinus* most likely due to low VPD (maximum 0.3 kPa). When VPD increases again after November 1$^{\text{st}}$ only *Pinus* recovers from sap flow velocity depressions quicker. *Alnus*, on the contrary, remains comparably low (max 3.7 cm h^{-1}, figure 3.1). However, this effect is partly captured by the corresponding GLM analyses since the described period after the second label application (table A.2) is showing less dependency for VPD and soil moisture on sap flow velocity than GLM analyses during the periods of the first label application (e. g. table A.1).

Summarized we find for sap flow velocity a clear dependency on atmospheric conditions represented by vapor pressure deficit and a weaker dependency on soil water content. However, under very dry water limited conditions in the soils dependencies observed to change towards less importance for atmospheric conditions. These informations about water movements are important when analysing the movement of stable water isotope tracers and periods of movement in the tree pots.

3.3 *In-situ* stable water isotope measurements and their reaction to the tracer applications

In contrast to sap flow velocity, stable water isotope signals are influenced mainly by the experiment settings including label / irrigation applications. Hence, the impact of the two irrigation events with deuterated label water is clearly visible by increasing $\delta\ ^{2}H$ values with steps up to + 50 ‰$_{VSMOW}$ (figure 3.1). Values for $\delta\ ^{18}O$ on the other hand show not such a clear direct response to the label irrigation events, which is not surprising since $\delta\ ^{18}O$ remained unchanged for the label and irrigation water (−9 ‰, sd = 0.2 ‰). Nevertheless, all isotope probes capture a slow increase of $\delta\ ^{18}O$ values over time (R^2 = 0.45 – 0.72 for linear equations with positive inclination, figure 3.1).

However, results for stable water isotopes also show that added isotope label cannot be transferred directly to the isotope measurements in the probes. Thus, for almost all *in-situ* probes over all trees the measured isotope values are about 20 ‰ lower than the label's $\delta\ ^{2}H$ values (label 1: 41 ‰, label 2: 95 ‰, figure 3.1). Additionally, added labelling water (0.06 m^3 for label 1 and 0.04 m^3 for label 2) into the 0.5 m^3 soil pots is barley enough water to fully replace the not deuterated pre label event water. Hence, volumetric water content in the soils before the first labelling are mostly between 5 and 25 vol.% (figure 3.1) which could be transferred roughly to 0.05 m^3 – 0.25 m^3 water per soil pot. However, only the soil 30 cm probe for *Quercus* is an exception, when measured $\delta\ ^{2}H$ values are temporally equal to the label water signal on 18th and 19th of September (figure A.13). Such high $\delta\ ^{2}H$ are very seldom and can be caused by labelling water directly hitting the isotope probes.

Towards the end of the experiment, starting with October 26th, decreasing trends in $\delta\ ^{2}H$ and $\delta\ ^{18}O$ values for *Alnus* and *Pinus* can be observed, even though no external isotope influences were present. Here, increasing water stress (water potential in the root bale for *Alnus* > 4 pF) accompanies relatively low vapor pressure deficit and sap flow velocities (figure 3.1). Since older water has a lighter deuterium signature ($\delta\ ^{2}H <= 41$ ‰) than label 2 ($\delta\ ^{2}H = 95$ ‰), this period could show a shift towards increasing influence of older water.

In the contrary, *in-situ* $\delta\ ^{2}H$ measurements at the beginning of the experiment, which are not effected by labelling events, show stable water isotope signatures closer to pre experiment precipitation than irrigation tap water (20 mm, four days before experiment start). Thus, *in-situ* measurements show values about −30 ‰ to −5 ‰ for $\delta\ ^{2}H$ (figure 3.1), while precipitation was on average $\delta\ ^{2}H = -28$ ‰ (sd = 15 ‰)

and irrigation water before experiment was $\delta\ ^{2}H = -63.1\,‰$). However, *in-situ* $\delta\ ^{18}O$ measurements at the experiment start (about $\delta\ ^{18}O = -8\,‰$) are closer to irrigation water used before the experiment ($\delta\ ^{18}O = -9.2\,‰$) than to precipitation ($\delta\ ^{18}O = -4\,‰$ (sd = 2 ‰)).

In terms of measurement accuracy all sensors show some clearly visible fluctuations, even for daily median values presented in figure 3.1. Taking into account higher temporal resolution (depending on sensors 2 – 4 hours), the δ value fluctuations for ^{2}H and ^{18}O become even more obvious and clearly exceed the theoretical measurement uncertainties for the ring-down laser spectrometer of ± 2 ‰ (figure 3.1 and figure A.11 to figure A.13). The *Alnus* xylem sensor at 270 cm height had repeating problems with water intrusion and therefore was deinstalled earlier.

Furthermore, heterogeneity of *in-situ* measurement results become visible when comparing different isotope probes within one tree pot (figure A.14 – figure A.16). Here, various probes differ the most in $\delta\ ^{2}H$ values just after labelling events (up to 41 ‰ within few days) but variation decreases clearly within two weeks. Also, differences between soil and tree probes can be explained by the temporal offset of the tracer arrival while variations within soil probes, also over longer time periods, have no simple explanation. Differences in soil isotope probes are suggesting heterogeneous soil conditions, which is supported by findings of soil moisture variations within one tree pot (figure 3.1). However, with increasing time after the labelling event, heterogeneity between *in-situ* probes within one tree pot decreases strongly with differences $< 5\,‰$ for *Alnus* and $< 20\,‰$ for *Pinus* and *Quercus* ate the end of label 1 or label 2 (end of the experiment). Here, more homogeneous isotope signal could be considered as one water pool throughout plant and soils.

Over the course of the experiment averaged root mean square differences between all isotope probes among a tree pot show that $\delta\ ^{2}H$ values for *Alnus* probes are more similar than values among *Pinus* or *Quercus* (average RMSD: *Alnus* = 12 ‰, *Pinus* = 17 ‰, *Quercus* = 14 ‰, figure 3.5). However, the differences between the trees are not significant according to an ANOVA test (p-value > 0.05).

In summary stable water isotopes are a clearly to detect and trace through the soil-plant continuum after tracer application. Furthermore, *in-situ* isotope measurements can be used to estimate sources of plant water uptake and water pools and distribution in the soils.

3.3.1 Using *in-situ* stable water isotope measurements to derive water travel times

In general, highest possible temporal resolution is used to compare sap flow velocity results with water travel velocity derived by the deuterium tracer (figure A.11 – figure A.13). Results show that the increase of the deuterium signal happens for most of the *in-situ* isotope soil and xylem probes at 15 cm height faster than temporal resolution (about 2 – 10 hours; table 3.1, table A.5 and figure A.11 – figure A.13).

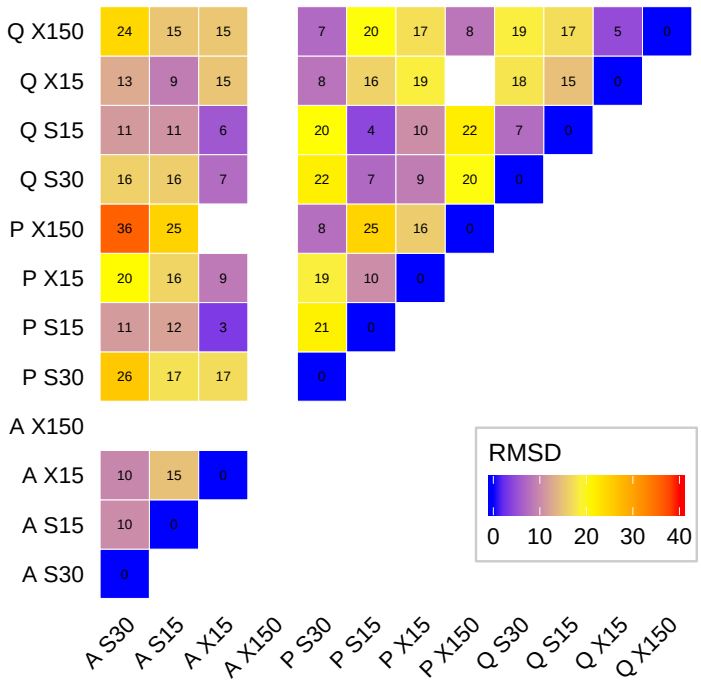

Figure 3.5: Root mean square differences (RMSD) between the different *in-situ* stable isotope probe locations and trees. For calculation purpose, measurements were summarized to median daily values and RMSD was only calculated for those days with measurements.

However, not all isotope probes show expected responses to the labelling / irrigation events. Thus, soil probes for *Alnus* (15 cm) and *Pinus* (30 cm) show no clear δ ^{2}H increase after the labelling (table 3.1). Also, the tracer response for the higher xylem sensors is generally less clear to see and associated with a slow increase over time. Furthermore, the first labelling event shows visible responses in more isotope probes than the second labelling event does during which some probe failures occurred as well (table 3.1 and table A.5).

To calculate water travel velocities within the tree, only the lower isotope probes in the stems were used because tracer arrival was better to detect here, compared to the upper stem isotope probes. Water travel velocities derived from isotope data was approached by dividing minimum flow length (assumed as probe height) through tracer travel time presented in table 3.1 and table A.5. Since actual flow paths from water uptake to the lower stem isotope probes (15 cm) are likely to be longer than 15 cm and tracer arrival might have already happened before the actual measurement took place. Therefore the result is referred to a minimum water travel velocity.

Table 3.1: Schematic tracer response analysis for the first labelling event. Responses for deuterium tracer were calculated by using a visual approach of looking at each single data point. Some isotope probes show clear tracer arrival with the first measurement after tracer application (*) whereas other isotope probes show tracer responses with later measurements (+). See table A.5 in the appendix for the results of the second labelling event.

tree	sensor	response delay time and change of δ ^{2}H values in [‰$_{VSMOW}$]
Alnus	soil 30 cm	within 2 days$^{+\ -}$: +22 (-32 -> -10)
Alnus	soil 15 cm	no direct increase: slow increase until next label event
Alnus	xylem 15 cm	within 4 hours*: no change; (within 21 hours^{+}: +28 (-28 -> 0))
Alnus	xylem 150 cm	no direct increase: steady increase until sensor failure
Pinus	soil 30 cm	no direct increase: unclear
Pinus	soil 15 cm	within 25 hours*: +25 (-30 -> -5)
Pinus	xylem 15 cm	within 1 hour*: no change; (within 17 hours^{+}: +17 (-12 -> 5))
Pinus	xylem 150 cm	no direct increase: slow steady increase until sensor failure
Quercus	soil 30 cm	within 2 hours*: + 28 (-25 -> 3)
Quercus	soil 15 cm	within 24 hours^{+}: +50 (-24 -> 26)
Quercus	xylem 15 cm	no direct increase: slow increase until next label event
Quercus	xylem 150 cm	no direct increase: slow steady increase until sensor failure

Note: *first measurement after label; $^{+}$ not first measurement after label; $^{-}$ mayor failure

Here, fastest minimum velocities are calculated for *Quercus* (5 cm h^{-1}) during the second labelling event (table A.5). For the first labelling event (table 3.1) minimum velocities estimated are lower, suggesting faster velocities than 0.7 cm h^{-1} for *Alnus* and 0.9 cm h^{-1} for *Pinus*. Assuming the temporal resolution of 17 or 21 hours represents almost one day, these findings are close to average daily sap flow velocities during the first labelling event (*Alnus* = 1.9 cm h^{-1}, *Pinus* = 1.9 cm h^{-1}). Results for the first labelling event are summarised in table 3.2.

Unlike water travel velocities derived from sap flow velocity sensors, water travel velocities derived from isotope signals give a hint about the velocity variation. Different water travel velocities for a single water particle could give a hint for different long flow paths and possible temporal water storages. Direct measured sap flow velocity on the contrary show very similar results within one tree for the upper and lower stem sensor. Thus, dispersion processes of the actual water travel time from the root towards the stem remains unknown.

3.4 Effects on water travel velocity derived from stable water isotope signals

While water travel velocities derived from sap flow velocity is influenced mainly by atmospheric conditions (section 3.2), water travel velocities derived from stable water

Table 3.2: Average daily water travel velocity for sap flow velocity sensor and water travel velocity derived from isotope signal based on tracer travel times shown in table 3.1. Results for both methods are based on the same dates shortly after the first labelling event (09.17.19). Due to sensor failures and tracer dispersion only *Alnus incana* and *Pinus pinea* at the lower xylem isotope probes (15 cm) are considered.

	Alnus	*Pinus*
sap flow velocity sensor [$\mathrm{cm\,h^{-1}}$]	1.9	1.9
stable isotope probes [$\mathrm{cm\,h^{-1}}$]	0.7	0.9

isotope signals show no clear influence by atmospheric or soil conditions (figure 3.6). Correlation analysis using Kendall rank correlation show absolute Kendall's τ values smaller than 0.46 (figure 3.6) for all correlation analysis between δ isotope values of isotope probes and sap flow velocities, soil moisture or VPD data. Although some correlations are significant (p-value < 0.05) according to a Kendall correlation test, it is hard to detect the one single driving parameter. Additionally, for most isotope probes versus sap flow velocity or soil moisture measurements trends are contrary for $\delta\ ^{2}\mathrm{H}$ and $\delta\ ^{18}\mathrm{O}$.

Leaving out the soil-, tree- and atmospheric conditions as driving parameters for the isotope signals, we suggest the added deuterated irrigation (label) water to be a determining factor of stable water isotope values measured in the stable water isotope probes.

3.5 Comparing *in-situ* stable water isotope measurements with commonly used destructive measurement methods

Considering the variances and fluctuations of *in-situ* isotope measurements (section 3.3), it is partly difficult to find a representative value compare results from *in-situ* observation to destructive measurements. In general, destructive measurements show a wider spread within one tree pot than *in-situ* measurements.

Average differences for results from destructive and three days median *in-situ* measurements display clear offsets destructive and *in-situ* methods (for $\delta\ ^{2}\mathrm{H}$: 2 ‰ to 14 ‰, for $\delta\ ^{18}\mathrm{O}$: 0.4 ‰ to 5.2 ‰, figure 3.7 and figure A.17). For $\delta\ ^{2}\mathrm{H}$ values, 63 % of the destructive measurements are found outside of the *in-situ* measurement 95 % confidence interval when considering a three days timeslot (centralized on the destructive measurement campaign day). On average, δ values for both stable isotopes, but in particular for $^{18}\mathrm{O}$, are more positive for destructive measurements than for *in-situ* measurements (figure 3.7 and figure A.17).

Comparing the calculated offsets between destructive and *in-situ* measurements for $^{2}\mathrm{H}$, we found significant differences among the four different measure-

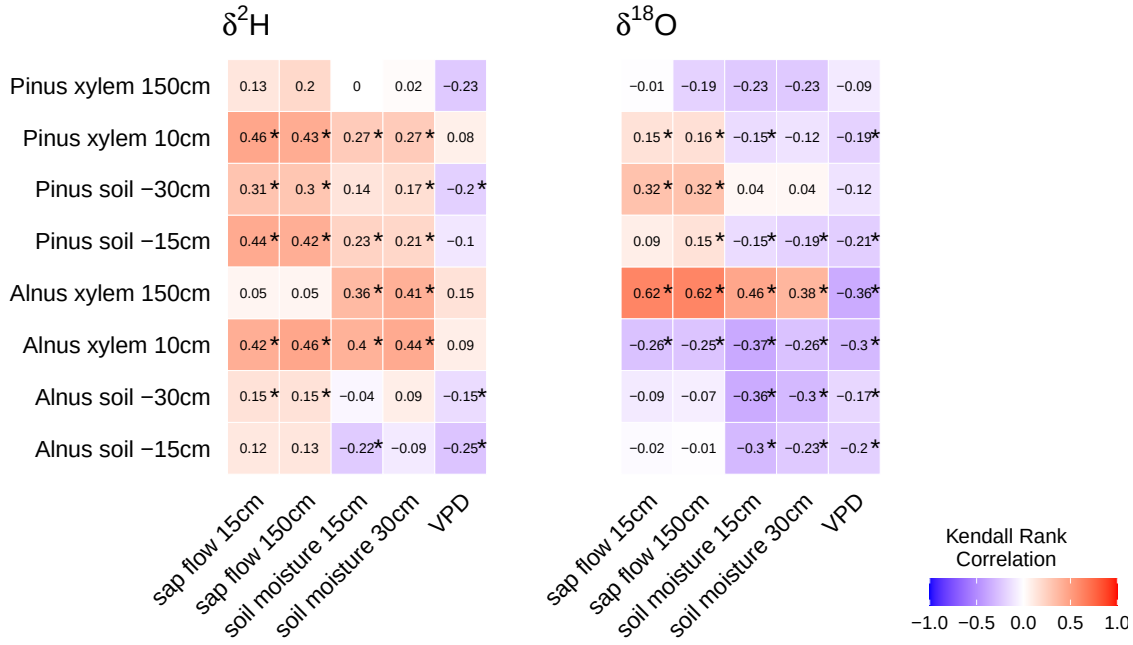

Figure 3.6: Pairwise Kendall correlation test for results of *in-situ* isotope probes against sap flow velocity measurements at 15 cm and 150 cm for *Alnus incana* and *Pinus pinea*.*Quercus suber* was excluded due to sap flow velocity sensor failure. Vapor pressure deficit (VPD) is derived from data of the German weather station close by (1 km).
Note: * shows significant correlations according to Kendal correlation test (p-values < 0.05)

ment campaigns (ANOVA, p-values < 0.05). However, comparing differences between methods grouped among tree species or measured material (xylem or soil) no significant differences can be found (figure A.18). Additionally, both used destructive methods, cryogenic vacuum extraction and direct water vapor equilibration, show clearly different results for δ ^{2}H values. Average differences of δ ^{2}H values between both methods are 13 ‰ for soil samples and 11 ‰ for xylem samples.

Furthermore, when comparing results for δ ^{18}O of destructive versus *in-situ* methods, a trend becomes visible over time (figure A.17). While for *in-situ* measurements an increasing trend is observed (figure 3.1), destructive measurements show a decreasing trend over time. Thus, δ ^{18}O signals decrease on average over all probes per tree pot at least by -2.69 ‰ for *Pinus* between the first and last measurement campaign (Δ *Alnus* $= -3.77$ ‰, Δ *Quercus* $= -4.26$ ‰). This leads to decreasing δ ^{18}O differences between measurement methods for later measurement campaigns, with differences smaller than $\pm$ 2.5 ‰ for measurement campaign three and four (figure A.17 and figure A.19).

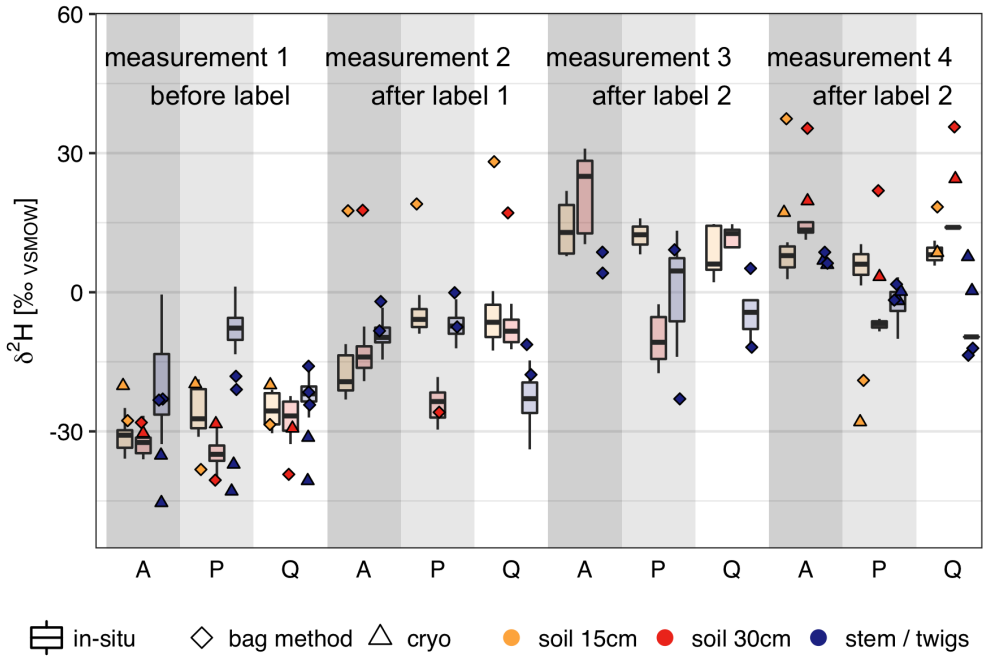

Figure 3.7: Comparison of destructive isotope measurement methods (Direct water vapor equilibration = bag method, Cryogenic vacuum extraction = cryo) with *in-situ* isotope measurement for the water isotope deuterium in δ notation. Box plots (with median) represent *in-situ* measurements for a three days time frame around the destructive measurement campaigns. Dates of measurement campaigns and applied methods can be found in table 2.4.
Letters at x-axis refer to the trees: A = *Alnus incana*, P = *Pinus pinea*, Q = *Quercus suber*. Comparison of δ ^{18}O results can be found in figure A.17 in the appendix.

In contrast to *in-situ* δ ^{18}O measurements, samples extracted via destructive measurements suggest a higher influence of pre experiment precipitation water (δ ^{18}O $= -4.2\,‰$, sd $= 2.3\,‰$, section 3.3) during the time before the labelling events. However, these findings for the first measurement campaign are not consistent with results for δ ^{2}H values (figure 3.7) which shows average δ values for destructive measurements more negative than δ values for *in-situ* measurements (figure A.18). It is notable that δ ^{18}O variability within one tree is much higher for destructive measurements than for *in-situ* measurements.

In summary we observe partly different results of δ ^{18}O and δ ^{2}H when comparing destructive with *in-situ* isotope measurement methods but in general results between methods are comparable. Possible explanations for differences between both stable water isotope need to be discussed, including the importance of present rain and irrigation water which have different isotope signatures.

4 Discussion

4.1 Dependency on tree and soil properties

Using stable water isotope tracers is highly motivated by the possibility to better understand plant based water uptake and usage processes. However, almost all new understanding in ecohydrology based on stable water isotopes assume that stable water isotopes are a conservative ideal tracer in the soil – plant – atmosphere continuum. Although, stable water isotopes are mostly accepted as ideal tracers (Ehleringer and Dawson, 1992; White et al., 1985, and many more), an increasing number of recent studies is questioning this assumption (Ellsworth and Sternberg, 2015; Ellsworth and Williams, 2007; Poca et al., 2019). However, this study does not claim to contribute directly to this very specific question but suppose that future studies with *in-situ* measurement systems could do so.

So far, the used *in-situ* measurement method by Volkmann and Weiler (2014) is applied in soils (Volkmann and Weiler, 2014) and a limited number of tree species (sessile oak, European beech and maple trees) only (Volkmann et al., 2016a,b). Thus, this study gives the opportunity to double the number of tested species by using an alder, pine and cork oak tree. However, all tree species used here vary strongly in the xylem and stem wood structure. This should be considered for stable isotope measurements. Hence, water conductivity in tree stems depends highly on vessel structure and diameter and different responses in sap flow. Thus, theoretical sap flow can be higher for wider vessels in the xylem structure, according to the Hagen-Poisenille equation. All these factors potentially can influence tracer distribution.

Conifer's xylem structure, including *Pinus pinea*, is fibres free and therefore dominated by tracheids which fill up to 90 % of a xylem cross section for transport water up to the crown (Hacke, 2015).

In contrast, hardwood's wood structure is more complex in comparison with conifers. Here, the wood consists of tracheas (vessels) for nutrition and water transport and of wood fibre for stabilisation purpose. Vessels are twisting non parallel cell structures in the stem which establish connections when two vessels touch each other (Kadereit et al., 2014; Orians et al., 2004). However, in a more detailed view both hardwoods used here still differ notable in their wood structure.

Quercus suber, cork oak, is a semi-ring porous tree which is adapted to dry Mediterranean conditions with temporal water scarcity (Barij et al., 2011; Leal et al., 2007). The wood consists of non transport active heartwood and sapwood for water transport. In sapwood the vessel size increases with cambial age which applies in particular for large vessel sizes. Still, regardless of the vessel size distribution, the number of vessels does not change over years (Barij et al., 2011; Leal et al., 2011). Although, *Quercus suber* has rather small vessels compared to other closely related

species the wood water content is still about 60 % in sapwood and heartwood (Barij et al., 2011).

Furthermore, abiotic factors, such as drought, play an important role for oak trees, when influencing the building of earlywood during the start of growing season (Fonti and García-González, 2008). This applies because earlywood in semi ring-porous tree species, like *Quercus suber*, is the zone with comparable larger vessel pores and therefore is crucial for water transport capacity (Kadereit et al., 2014, p. 126).
The influences of cork harvest indicated in literature are negligible here because the tree remained unharvested.

Alnus incanca, on the contrary, is a sapwood tree which means heartwood cant be detected. Moreover, *Alnus* has a diffuse porous vessel distribution with equally distributed vessels among earlywood and latewood (Kadereit et al., 2014). In conclusion, it can be expected that water transport towards the leaves, and therefore also the tracer, is rather similar throughout the entire sapwood cross section.

We speculate that observing stable water isotopes with *in-situ* probes by Volkmann and Weiler (2014) could be easier in non-porous (conifers) and diffuse porous wood structure because the water flow passing the probes is more homogeneous. Likewise, the amount of heartwood, and therefore the tree age, could be crucial for stable water isotope measurement.

Furthermore, from a tree physiologically perspective the most active stem tissues are known to have the highest water contents (Schepper et al., 2012). Considering trees used here, the most active sap flow is likely to be found in the sapwood around 1 cm below the cambium while the sap flow inactive heartwood starts about 3 cm inside the cambium (Caylor and Dragoni, 2009; Cohen et al., 2007). Similar results are observed in our sap flow measurements with almost no water movement in 3 cm depth from the cambium. This leads to the conclusion that at least 2 cm of the 5 cm long *in-situ* isotope probes are located in wood tissue without water movement and thus, without contact to labelling / tracer water.

According to the described tree physiology properties influences on *in-situ* measurements are likely to expect. Especially (semi) ring-porous vessel distribution could cause heterogeneous water transport velocities and volumes among a sapwood cross section. However, our observation of tracer responses in *Quercus* only show, if at all, a very slow water transport. We suspect that multiple factors might be responsible: First, the cork oak is a relatively young tree (about 20 years) and second the water transport increases detectable with tree age (Leal et al., 2011). Third, the tree might suffer from abiotic and biotic influences, visible in a relative low amount of leaves. Thus, climate condition were not like Mediterranean condition and the tree was louse infested just before the experiment start.

However, the numbers of tested species is still very limited with high limitation of sufficient replications. Consequently, we strongly suggest establishing more studies with higher numbers of replication under controlled condition, if possible. Also, we suggest further investigation of how this probe installation set-up influences stable water isotope measurements or whether isotope probes can be installed in sap flow active locations only.

Other *in-situ* measurement uncertainties might be caused due to installation difficulties when the phloem is not removed completely. The phloem is used by the tree to transport sugars from the leaves downwards to the roots and thus has a different stable water isotope signature than sapwood including issues with organic contaminations. Thus, for the alnus tree we were able to observe temporally brownish liquid water intruding the isotope probes. We hypothesised that it would be sugary water flowing downwards in the phloem and therefore built up enough water pressure to intrude the isotope probes. This is possible because the *in-situ* probes are only hydrophobic and not waterproof. Another entering path for external liquid waters could be connections that are not completely sealed, especially those parts sealed with glue. However, leaking connections are unlikely although Volkmann et al. (2016b) note that the probe design is not fully perfect, yet.

Liquid water intruding the gas tubes occurred most likely after irrigation / labelling events. This is probably due to higher water availability after a period of water scarcity which is resulting in high tree activity. Since all probes are connected via the valve boxes entering water would contaminate the entire tubing system. Hence, the consequences are time consuming drying and cleaning data gaps that are in visible figure 3.1. Unfortunately, data gaps would happen during time periods of high investigative interest in stable water isotope data. We therefore would recommend a different connection / valve – tube system which reduces the probability of spreading the contamination among other probes.

Similar to sap flow sensors, *in-situ* isotope probes cause wounding to the tree, too. Thus, wounded xylem may be bypassed by tree water when vessels become inactive due to damages (Hacke, 2015). In a not published study this was especially visible for sap flow sensors installed in cork oaks in a natural environment in Portugal. Here, a notable amount of sap flow sensors showed zero sap flow velocity although outer appearance suggested normal tree conditions.

Another important role in root water uptake and therefore tracer input in the tree system plays soil properties and root distribution. Hence, irrigation water is likely to follow preferential flow paths rather than distribute homogeneous within the tree pots to guaranty equal isotope signals around each active root (Allen et al., 2019; Benettin et al., 2019; Beven and Germann, 1982, 2013). We further speculate that roots growth limitation to a small root bale before the experiment influences natural root distribution and therefore spatial water uptake. This is visible in differences

of water related soil conditions (soil metric potential and soil moisture) between the root bale soil and the added silty soil (figure 3.1). Thus, for instance, Mahindawansha et al. (2018) show that plant water uptake for rice plants is related to root length density in constant water content among depths. Furthermore, different root lengths influence flow path lengths and therefore the time until tracer arrival in the xylem isotope probes (Kirchner et al., 2001).

4.2 *In-situ* isotope measuring precision and necessary data processing

Accuracy and reliability of the standards is crucial when using the *in-situ* method by Volkmann and Weiler (2014). Therefore, only by using the standards that are actually measured, vapor isotopes ratios can be transformed to liquid water isotope ratios. However, stable water isotopes ratios in δ values across a water phase transition are known to depend on humidity (Bastrikov et al., 2014) and temperature (Majoube, 1971). These phase transitions occur for *in-situ* measurements when measuring the liquid phase indirectly via the vapor phase, assuming these two phases are in an equilibrium.

Regarding our vapor isotope measurements, we observe daily variation in humidity which mostly responses, as expected, opposite to the daily air temperature variation (Allen et al., 2004; Lawrence, 2005). However, exact temperature or humidity condition in the probes itself remain unknown. Therefore, measuring standards which are placed under similar conditions as xylem or soil probes can reduce temperature and humidity influences on the final results.

Nevertheless, measurements in this study shown in figure A.11 to figure A.13 are far less consistent than results by (Volkmann et al., 2016b), especially for $\delta\ ^{18}O$ values. Thus, results show higher variabilities of isotope measurements when low changes of δ isotope values are expected. Unlike our first assumption, changing the standards' δ values, for instance at a fixed value, does not improve general results. Furthermore, different standards show different isotopic trends over time which are clearly not related to each other (figure 4.1 A). Also median δ values per hour after humidity correction show no daily routine (figure 4.1 B), confirming the successful approach of humidity correction for isotope measurements. Furthermore, the temperature among all soil and water standards is very similar and mostly consistent with the temperature measured in the tree pots' soils (figure 4.3). Consequently, an important criterion for using the standards is fulfilled. Additionally, water loss in soil standards due to evaporation seem to be low according to soil moisture measurements (about 1 %, figure 4.2).

Although, the influences of the standards on the results are lower than expected, the *in-situ* measurement method highly relies on correct standard applications. Moreover, Volkmann et al. (2016b) suggest further research on temperature influences in the probes.

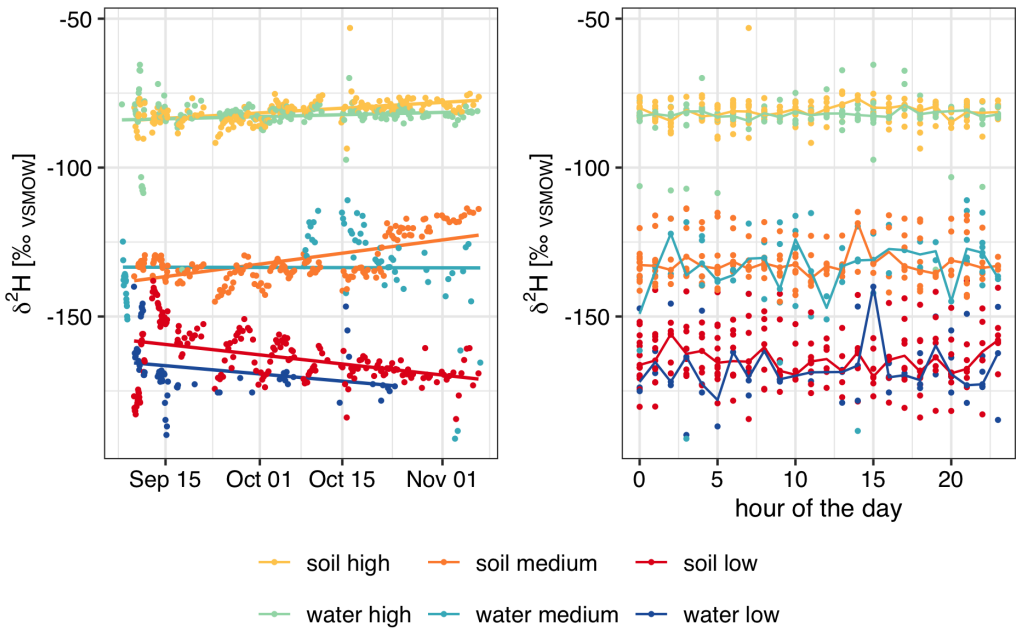

Figure 4.1: A: δ ^{2}H values for soil and water standards monitored with *in-situ* isotope probes. The lines indicate the linear trend over the time. Single outliers are not removed because they are less powerful when all standards are used together for transferring soil and xylem probe measurements.
B: Measurements of A grouped according to measurement hour during the day. Lines connect median values for each hour and standard. Note that some hours coincidently contain very few measurements which results in high influences on hourly median value. Results for δ ^{18}O values are found in figure A.20 in the appendix.

Summarizing, in this study no obvious advantage for one type of standard, soil or water, is found. We rather suggest using a sufficient replication of standards including further investigation on measurement behaviour and influence of standards on general results under field conditions. Thus, our standards showed rather unexpected trends over time including isotopic enrichment or opposing trends although all standards were treated equally.

Other crucial problems are condensation or liquid in the measurement tubes and valve boxes. This is because liquid water is known to have a different isotope signal than vapor (Majoube, 1971) and because the Picarro cannot measure humidities that are too high. Furthermore, measurement accuracy of the Picarro depends on humidity, too.

By applying post data processing, we are able to easily detect and correct errors related to variation in humidity. Uncertainties due to the usage of standards can be detected but applying an accurate correction remains challenging.

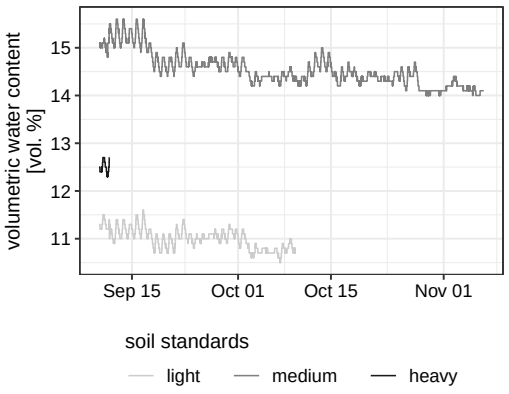

Figure 4.2: Volumetric water content for measurements in the soil standards. Note that different starting points are likely due to difficulties during installation.

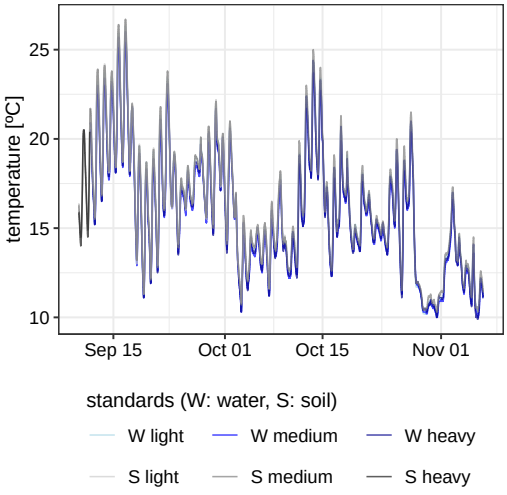

Figure 4.3: Temperature measurements for soil and water standards. Due to high similarity lines overly each other.

4.3 Water uptake strategies and tracer recovery rates

In general, more replications would be helpful to better evaluate water uptake strategies. However, *in-situ* stable isotope measurements are generally consistent with sap flow velocity or soil water content and metric potential in terms of tree activity. Thus, slow water travel times, as well as a weak decrease in soil water content, suggest low water consumption (figure 3.1). Here, our approach to calculate water travel times is showing promising results and can be improved when probe failure is reduced. Furthermore, high resolution data also could help to apply models or curve (e. g. Gompertz function) functions to find standardized parameters, such as mean travel velocities.

Considering the flow path estimation, water travel times derived from stable water isotopes are a comparable conservative estimation because root length are excluded from flow paths. As a result, water travel time is acceptable higher than presented in table 3.2. Additionally, water travel times derived from stable water isotopes possibly exceeds water travel times derived from sap flow velocity. Our speculations are confirmed by Meeinzer et al. (2006) who observed in conifers an underestimation of sap velocities derived from sap flow sensors compared with sap velocities derived from a $^{2}H^{2}O$ labelling experiments. In particular, this might be true for ring-porous tree species with bigger vessels of high flow rates (Hacke, 2015; Kadereit et al., 2014). However, even different trees of one species may also show high variation in sap flow velocities when site properties vary (Hassler et al., 2018).

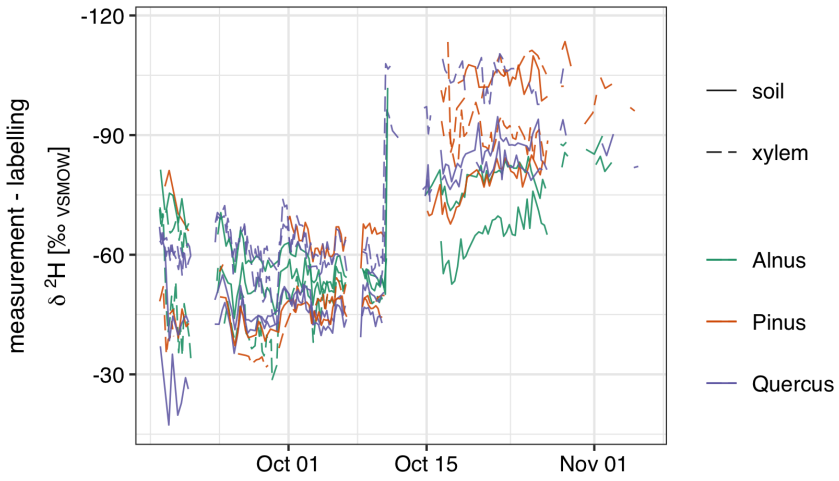

Figure 4.4: Differences between *in-situ* stable isotope measurement and the added labelling water for $\delta\ ^2H$ values only. Negative values describe how much lower results in isotope probes are compared with labelling $\delta\ ^2H$ values. Values for labelling are $\delta\ ^2H = 41\,‰$ (first label) and $\delta\ ^2H = 95\,‰$ (second label, from 10.10.19 onwards).

Measured tracer intensity or tracer recovery may give indications on water used by the trees. As pointed out in the results, *in-situ* isotope probes measure δ isotope values clearly lower than added labelling water (figure 4.4). Additionally, the offset of $\delta\ ^2H$ values is approximately similar for soil and xylem measurements after some equilibration time. We speculate that the soil isotope probes represent a mixture of older (lower $\delta\ ^2H$ values) and newer, meaning more deuterated, water. This mixture is likely to distribute, partly heterogeneous, among the entire soils in the tree pots. In conclusion his means that heterogeneous soil conditions and unequal distribution of irrigation water makes water uptake analysis per depths challenging.

Furthermore, we assume that the trees, excluding *Quercus*, take up the isotopic "mixture" of water rather than water associated to one pool described in the two water world hypothesis by McDonnell (2014). Thus, one crucial criteria for the two water world hypothesis is the offset of measured isotopic ratios in plant material compared to the local meteoric water line (McDonnell, 2014). However, linear regressions for our xylem *in-situ* results in the dual isotope plot do clearly not correspond to the local meteoric water line (figure A.21 – figure A.23) but this applies as well for soil measurements. Furthermore, linear regressions for xylem and soil isotope results are quite parallel in the dual isotope plot. This is possible supporting our assumption of one mixed water pool because isotope responses are similar in soil and xylem probes.

Comparing the isotope signal for *Alnus* and *Pinus*, havier isotope ratios are observed in the xylem probes in 15 cm compared with averaged soil isotope signal (figure 4.5 and table A.6). This can be shown during both labelling event plus the time period before the experiment. We suppose that transpiration through the bark

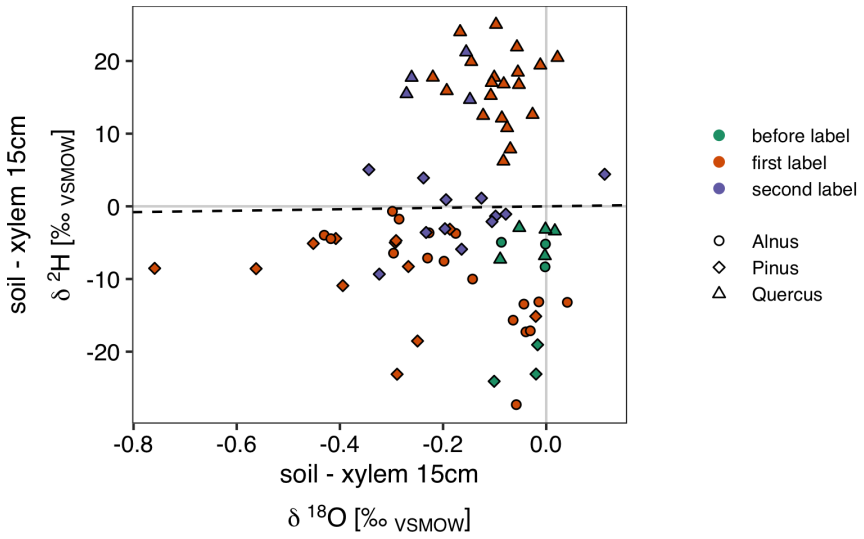

Figure 4.5: Differences between measured stable water isotopes in soil (averaged over both probes) and the lower xylem isotope probes at 15 cm stem height shown in dual isotope space. See figure A.24 for the upper xylem isotope probe compared with the soil probes. For reference, dashed line indicates 1:1 line.

could cause enrichment of heavier isotopes in the xylem water as also observed in other studies by Feakins and Sessions (2010); Oren and Pataki (2001) or Zhao et al. (2016).

Nevertheless, these finding do not hold for *Quercus* or the upper xylem isotope probes which show during the labelling experiment mostly lower δ ^{2}H values than the soil probes (figure A.24, table A.6). While in *Quercus* the missing water uptake is likely responsible, complex tissue structure or temporal water storages causing high dispersion are a possible explanations for the upper stem probes.

However, under very dry conditions with pF-values exceeding the PWP (figure 3.1) decreasing δ ^{2}H values are observed for soil and xylem sensors in *Alnus* and *Pinus*. We suppose that older (lighter) more bound water becomes visible in the isotope measurements. Probably the older water is more difficult to access for the trees and therefore is only visible in notable portions under water stress conditions. This is consistent with other studies which find an increasing proportion of bound water in total soil water under drought conditions which can cause a shift of stable water isotopes (Lu, 2016; Tuller and Or, 2005).

4.4 *In-situ* stable water isotope measurements in future ecohydrology

We have to admit that this study highlights a few disadvantages and measurement uncertainties for the used *in-situ* probes by Volkmann et al. (2016b). But do these arguments disqualify *in-situ* measurements with respect to common used method, such as cryogenic vacuum extraction? We would deny this! Thus, considering results regarding measurement accuracy also common used methods are highly discussed in terms of reliability, as for instance presented by Orlowski et al. (2018a) or Berry et al. (2017).

Comparing the *in-situ* method with the destructive methods, as proof of concept should be questioned (figure 3.7 & figure A.17 or figure A.18 & figure A.19). Instead, a better option could be to use different measurement methods parallel and then compare their final results. Consequently, similar trends over time can be observed by different methods although actual measurement results are not comparable. Nevertheless, here we want to highlight the advantages and importance of *in-situ* stable water isotope measurements, regardless of the specific *in-situ* method.

However, further investigations should be applied to determine reasons for differences in destructive and *in-situ* methods, especially because $\delta\ ^{2}H$ and $\delta\ ^{18}O$ in our experiment show different trends. So far, we assume two possible explanations: first, by chance different old waters with different isotopic signals are measured or second, the trends that are relatively easy to detect are due to unknown reasons related to the measurement system. This could include evaporation fractioning during destructive sampling processes caused by different weather conditions (air temperature, humidity) or different accessed water for measurements (e. g. different portion of bound water). However, opposing offsets for $\delta\ ^{2}H$ and $\delta\ ^{18}O$ between the different measurement methods are hard to explain through this argumentation.

Additionally, it should be considered that destructive bag method (Wassenaar et al., 2008) and *in-situ* method (Volkmann et al., 2016b) both rely on vapor equilibrium measurements and therefore are methodically very similar. However, results comparing destructive and *in-situ* methods suggest more similarities between bag method and cryogenic vacuum extraction than bag method and *in-situ* method. Possible explanation could be influences during the sampling for destructive measurements.

Even so, reasons to use *in-situ* measurements are, in our point of view, obvious: e. g. low costs, easy handling once installed, heigh temporal resolution, no sample or experimental material consumption. Especially high temporal resolution measurements at the same location gives the opportunity for new investigations in ecohydrology. Therefore, we suggest that in particular processes in small time scales, like temporal water storages in tree stems, or temporal adjustment to abiotic factors in root water uptake patterns can take advantages of *in-situ* methods (Barbeta et al.,

2020; Schepper et al., 2012; Vargas et al., 2017). This may especially gain importance when plants and trees are facing new challenges in water management due to changing climate. Furthermore, better understanding of fractioning processes in plants or soils could be archived by *in-situ* monitoring, especially since fractioning processes are happening in small time scales but therefore have a relatively high impact on isotope tracer experiments (Benettin et al., 2019; Orlowski et al., 2018b).

5 Conclusions and Outlook

This thesis presents results from a semi-controlled isotope labelling experiment with three different trees (*Alnus incana*, *Pinus pinea* and *Quercus suber*). We used an *in-situ* measurement approach with high temporal resolution which, so far, is not much in use. By using deuterated water as a tracer we are able to locate the labelled irrigation water through the soil-tree continuum due to a change in the measured stable water isotope composition. Increases of δ ^{2}H values are similarly observed for *in-situ* and destructive measurement methods over the course of the experiment. However, δ ^{18}O show opposing trends for *in-situ* and destructive measurements over the course of the experiment although δ ^{18}O values in labelling water remained unchanged. We highly suggest more investigation on differences between *in-situ* and destructive measurements also to better understand what causes differences.

Furthermore, δ ^{2}H results by the tracer experiment can be used for estimating water travel times from the soils into the tree xylem. Here, we are able to measure water travel times similar velocities observed in sap flow velocity sensors. However, *in-situ* stable water isotope measurements are capable to hold more information than sap flow velocity regarding water travel speed distribution or temporal water storages. This also includes investigations about plant specific water uptake strategies.

By monitoring soil conditions, sap flow velocity and stable water isotopes we are able to compare and relate different properties of ecohydrology to each other. Across all probes and sensors we observe similar responses within one tree pot but partly clear differences between tree species. Thus, high tree activity in terms of sap flow velocity is visible in comparable fast tracer travel times and a notable faster decrease of soil water content. Among the three trees *Alnus incana* and *Pinus pinea* are clearly more active and water transpiring than *Quercus suber*.

We conclude that advantages of *in-situ* methods should be obvious especially if considering recently discovered uncertainties for destructive measurement methods. Generating millions of stable water isotope measurements without no man power included is just another huge advantage. However, *in-situ* methods are infrequently used but we hope for a change soon.

Additionally, *in-situ* isotope measurements potentially can help to better understand future ecohydrological research questions especially related to locally limited processes in short time scales such as temporally water storage in stems or water loss and uptake through the bark. Furthermore, *in-situ* methods could be helpful to proof or reject the two water world hypothesis and investigation regarding isotope fractioning issues *in-situ*. Nevertheless, in our experiment we did not find evidence for the two water world hypothesis but we have to admit that soil and precipitation routines were far from systems where two distinguishable water pools were found.

Bibliography

Allen, R.G., Pereira, L.S., Raes, D., Smith, M., 2004. Crop evapotranspiration: Guidelines for computing crop water requirements (FAO Irrigation and Drainage Papers). Food and Agriculture Organization of the United Nations (FAO).

Allen, S.T., Kirchner, J.W., Braun, S., Siegwolf, R.T.W., Goldsmith, G.R., 2019. Seasonal origins of soil water used by trees. Hydrology and Earth System Sciences 23, 1199–1210. doi: 10.5194/hess-23-1199-2019.

Allison, G., Hughes, M., 1983. The use of natural tracers as indicators of soil-water movement in a temperate semi-arid region. Journal of Hydrology 60, 157–173. doi: 10.1016/0022-1694(83)90019-7.

Almeida, J., Barbosa, L., Pais, A., Formosinho, S., 2007. Improving hierarchical cluster analysis: A new method with outlier detection and automatic clustering. Chemometrics and Intelligent Laboratory Systems 87, 208–217. doi: 10.1016/j.chemolab.2007.01.005.

Araguás-Araguás, L., Rozanski, K., Gonfiantini, R., Louvat, D., 1995. Isotope effects accompanying vacuum extraction of soil water for stable isotope analyses. Journal of Hydrology 168, 159–171. doi: 10.1016/0022-1694(94)02636-p.

Barbeta, A., Gimeno, T.E., Clavé, L., Fréjaville, B., Jones, S.P., Delvigne, C., Wingate, L., Ogée, J., 2020. An explanation for the isotopic offset between soil and stem water in a temperate tree species. New Phytologist (online first). doi: 10.1111/nph.16564.

Barij, N., Čermák, J., Stokes, A., 2011. Azimuthal variations in xylem structure and water relations in cork oak (Quercus suber). IAWA Journal 32, 25–40. doi: 10.1163/22941932-90000040.

Bastrikov, V., Steen-Larsen, H.C., Masson-Delmotte, V., Gribanov, K., Cattani, O., Jouzel, J., Zakharov, V., 2014. Continuous measurements of atmospheric water vapour isotopes in western Siberia (Kourovka). Atmospheric Measurement Techniques 7, 1763–1776. doi: 10.5194/amt-7-1763-2014.

Benettin, P., Queloz, P., Bensimon, M., McDonnell, J.J., Rinaldo, A., 2019. Velocities, Residence Times, Tracer Breakthroughs in a Vegetated Lysimeter: A Multitracer Experiment. Water Resources Research 55, 21–33. doi: 10.1029/2018wr023894.

Berry, Z.C., Evaristo, J., Moore, G., Poca, M., Steppe, K., Verrot, L., Asbjornsen, H., Borma, L.S., Bretfeld, M., Hervé-Fernández, P., Seyfried, M., Schwendenmann, L., Sinacore, K., Wispelaere, L.D., McDonnell, J., 2017. The two water worlds

hypothesis: Addressing multiple working hypotheses and proposing a way forward. Ecohydrology 11, e1843. doi: 10.1002/eco.1843.

Beven, K., Germann, P., 1982. Macropores and water flow in soils. Water Resources Research 18, 1311–1325. doi: 10.1029/wr018i005p01311.

Beven, K., Germann, P., 2013. Macropores and water flow in soils revisited. Water Resources Research 49, 3071–3092. doi: 10.1002/wrcr.20156.

Blume, H.P., Brümmer, G.W., Horn, R., Kandeler, E., Kögel-Knabner, I., Kretzschmar, R., Stahr, K., Wilke, B.M., 2010. Scheffer/Schachtschabel: Lehrbuch der Bodenkunde. Springer Berlin Heidelberg. doi: 10.1007/978-3-662-49960-3.

Brand, W.A., Geilmann, H., Crosson, E.R., Rella, C.W., 2009. Cavity ring-down spectroscopy versus high-temperature conversion isotope ratio mass spectrometry; a case study onδ2h andδ18o of pure water samples and alcohol/water mixtures. Rapid Communications in Mass Spectrometry 23, 1879–1884. doi: 10.1002/rcm.4083.

Brooks, J.R., Barnard, H.R., Coulombe, R., McDonnell, J.J., 2010. Ecohydrologic separation of water between trees and streams in a Mediterranean climate. Nature Geoscience 3, 100–104. doi: 10.1038/ngeo722.

Brutsaert, W., 2014. Hydrology An Introduction. Cambridge University Press. URL: https://www.ebook.de/de/product/3270950/wilfried_brutsaert_hydrology.html.

Burgess, S.S.O., Adams, M.A., Turner, N.C., Beverly, C.R., Ong, C.K., Khan, A.A.H., Bleby, T.M., 2001. An improved heat pulse method to measure low and reverse rates of sap flow in woody plants. Tree Physiology 21, 589–598. doi: 10.1093/treephys/21.9.589.

Caldwell, M.M., Dawson, T.E., Richards, J.H., 1998. Hydraulic lift: consequences of water efflux from the roots of plants. Oecologia 113, 151–161. doi: 10.1007/s004420050363.

Campbell, G.S., Calissendorff, C., Williams, J.H., 1991. Probe for Measuring Soil Specific Heat Using A Heat-Pulse Method. Soil Science Society of America Journal 55, 291–293. doi: 10.2136/sssaj1991.03615995005500010052x.

Caylor, K.K., Dragoni, D., 2009. Decoupling structural and environmental determinants of sap velocity: Part I. Methodological development. Agricultural and Forest Meteorology 149, 559–569. doi: 10.1016/j.agrformet.2008.10.006.

Coenders-Gerrits, A.M.J., van der Ent, R.J., Bogaard, T.A., Wang-Erlandsson, L., Hrachowitz, M., Savenije, H.H.G., 2014. Uncertainties in transpiration estimates. Nature 506, E1–E2. doi: 10.1038/nature12925.

Cohen, Y., Cohen, S., Cantuarias-Aviles, T., Schiller, G., 2007. Variations in the radial gradient of sap velocity in trunks of forest and fruit trees. Plant and Soil 305, 49–59. doi: 10.1007/s11104-007-9351-0.

Cohen, Y., Fuchs, M., Green, G.C., 1981. Improvement of the heat pulse method for determining sap flow in trees. Plant, Cell and Environment 4, 391–397. doi: 10.1111/j.1365-3040.1981.tb02117.x.

Decagon Devices, 2007. 5TE Waer Content, EC and Temperature Sensors. version 6 Ed.

Dormann, C.F., 2013. Parametrische Statistik. Springer Berlin Heidelberg. doi: 10.1007/978-3-642-34786-3.

Dormann, C.F., Elith, J., Bacher, S., Buchmann, C., Carl, G., Carré, G., Marquéz, J.R.G., Gruber, B., Lafourcade, B., Leitão, P.J., Münkemüller, T., McClean, C., Osborne, P.E., Reineking, B., Schröder, B., Skidmore, A.K., Zurell, D., Lautenbach, S., 2012. Collinearity: a review of methods to deal with it and a simulation study evaluating their performance. Ecography 36, 27–46. doi: 10.1111/j.1600-0587.2012.07348.x.

Dubbert, M., Caldeira, M.C., Dubbert, D., Werner, C., 2019. A pool-weighted perspective on the two-water-worlds hypothesis. New Phytologist 222, 1271–1283. doi: 10.1111/nph.15670.

Dubbert, M., Cuntz, M., Piayda, A., Werner, C., 2014. Oxygen isotope signatures of transpired water vapor: the role of isotopic non-steady-state transpiration under natural conditions. New Phytologist 203, 1242–1252. doi: 10.1111/nph.12878.

Dubbert, M., Kübert, A., Werner, C., 2017. Impact of Leaf Traits on Temporal Dynamics of Transpired Oxygen Isotope Signatures and Its Impact on Atmospheric Vapor. Frontiers in Plant Science 8, Article 5. doi: 10.3389/fpls.2017.00005.

Ehleringer, J.R., Dawson, T.E., 1992. Water uptake by plants: perspectives from stable isotope composition. Plant, Cell and Environment 15, 1073–1082. doi: 10.1111/j.1365-3040.1992.tb01657.x.

Ellsworth, P.Z., Sternberg, L.S.L., 2015. Seasonal water use by deciduous and evergreen woody species in a scrub community is based on water availability and root distribution. Ecohydrology 8, 538–551. doi: 10.1002/eco.1523.

Ellsworth, P.Z., Williams, D.G., 2007. Hydrogen isotope fractionation during water uptake by woody xerophytes. Plant and Soil 291, 93–107. doi: 10.1007/s11104-006-9177-1.

Evans, J.R., Santiago, L.S., 2014. PrometheusWiki gold leaf protocol: gas exchange using LI-COR 6400. Functional Plant Biology 41, 223–226. doi: 10.1071/fp10900.

Evaristo, J., Jasechko, S., McDonnell, J.J., 2015. Global separation of plant transpiration from groundwater and streamflow. Nature 525, 91–94. doi: 10.1038/nature14983.

Feakins, S.J., Sessions, A.L., 2010. Controls on the D/H ratios of plant leaf waxes in an arid ecosystem. Geochimica et Cosmochimica Acta 74, 2128–2141. doi: 10.1016/j.gca.2010.01.016.

Fonti, P., García-González, I., 2008. Earlywood vessel size of oak as a potential proxy for spring precipitation in mesic sites. Journal of Biogeography 35, 2249–2257. doi: 10.1111/j.1365-2699.2008.01961.x.

Ford, C.R., Hubbard, R.M., Kloeppel, B.D., Vose, J.M., 2007. A comparison of sap flux-based evapotranspiration estimates with catchment-scale water balance. Agricultural and Forest Meteorology 145, 176–185. doi: 10.1016/j.agrformet.2007.04.010.

Froehlich, K., Gibson, J., Aggarwal, P., 2002. Deuterium excess in precipitation and its climatological significance (IAEA-CSP–13/P). Technical Report. International Atomic Energy Agency (IAEA).

Fuchs, S., Leuschner, C., Link, R., Coners, H., Schuldt, B., 2017. Calibration and comparison of thermal dissipation, heat ratio and heat field deformation sap flow probes for diffuse-porous trees. Agricultural and Forest Meteorology 244-245, 151–161. doi: 10.1016/j.agrformet.2017.04.003.

Gaj, M., Beyer, M., Koeniger, P., Wanke, H., Hamutoko, J., Himmelsbach, T., 2016. In situ unsaturated zone water stable isotope (2H and 18O) measurements in semi-arid environments: a soil water balance. Hydrology and Earth System Sciences 20, 715–731. doi: 10.5194/hess-20-715-2016.

Gat, J.R., Gonfiantini, R. (Eds.), 1981. Stable isotope hydrology : deuterium and oxygen-18 in the water cycle : a monograph prepared under the aegis of the IAEA/UNESCO Working Group on Nuclear Techniques in Hydrology of the International Hydrological Programme. International Atomic Energy Agency, Vienna.

Goldsmith, G.R., Muñoz-Villers, L.E., Holwerda, F., McDonnell, J.J., Asbjornsen, H., Dawson, T.E., 2012. Stable isotopes reveal linkages among ecohydrological processes in a seasonally dry tropical montane cloud forest. Ecohydrology 5, 779–790. doi: 10.1002/eco.268.

Gralher, B., Herbstritt, B., Weiler, M., Wassenaar, L.I., Stumpp, C., 2016. Correcting laser-based water stable isotope readings biased by carrier gas changes. Environmental Science & Technology 50, 7074–7081. doi: 10.1021/acs.est.6b01124.

Granger, C.W.J., 1969. Investigating Causal Relations by Econometric Models and Cross-spectral Methods. Econometrica 37, 424–438. doi: 10.2307/1912791.

Gutachterausschuss Forstliche Analytik, 2015. Handbuch Forstliche Analytik. nils könig Ed. URL: https://www.bmel.de/SharedDocs/Downloads/Landwirtschaft/Wald-Jagd/Bodenzustandserhebung/Handbuch/HandbuchForstanalytikKomplett.pdf?__blob=publicationFile.

Hacke, U. (Ed.), 2015. Functional and Ecological Xylem Anatomy. Springer International Publishing. doi: 10.1007/978-3-319-15783-2.

Hassler, S.K., Weiler, M., Blume, T., 2018. Tree-, stand- and site-specific controls on landscape-scale patterns of transpiration. Hydrology and Earth System Sciences 22, 13–30. doi: 10.5194/hess-22-13-2018.

Hawkins, D.M., 1980. Identification of Outliers. Springer Netherlands. doi: 10.1007/978-94-015-3994-4.

Hendry, M.J., Schmeling, E., Wassenaar, L.I., Barbour, S.L., Pratt, D., 2015. Determining the stable isotope composition of pore water from saturated and unsaturated zone core: improvements to the direct vapour equilibration laser spectrometry method. Hydrology and Earth System Sciences 19, 4427–4440. doi: 10.5194/hess-19-4427-2015.

Hendry, M.J., Wassenaar, L., 2009. Inferring Heterogeneity in Aquitards Using High-Resolution δD and δ^{18}O Profiles. Ground Water 47, 639–645. doi: 10.1111/j.1745-6584.2009.00564.x.

Herbstritt, B., Gralher, B., Weiler, M., 2012. Continuous in situ measurements of stable isotopes in liquid water. Water Resources Research 48, 1–6. doi: 10.1029/2011wr011369.

Hervé-Fernández, P., Oyarzún, C., Brumbt, C., Huygens, D., Bodé, S., Verhoest, N.E.C., Boeckx, P., 2016. Assessing the "two water worlds" hypothesis and water sources for native and exotic evergreen species in south-central Chile. Hydrological Processes 30, 4227–4241. doi: 10.1002/hyp.10984.

Jasechko, S., Sharp, Z.D., Gibson, J.J., Birks, S.J., Yi, Y., Fawcett, P.J., 2013. Terrestrial water fluxes dominated by transpiration. Nature 496, 347–350. doi: 10.1038/nature11983.

Junzeng, X., Qi, W., Shizhang, P., Yanmei, Y., 2012. Error of Saturation Vapor Pressure Calculated by Different Formulas and Its Effect on Calculation of Reference Evapotranspiration in High Latitude Cold Region. Procedia Engineering 28, 43–48. doi: 10.1016/j.proeng.2012.01.680.

Kadereit, J.W., Körner, C., Kost, B., Sonnewald, U., 2014. Strasburger - Lehrbuch der Pflanzenwissenschaften. Springer Berlin Heidelberg. doi: 10.1007/978-3-642-54435-4.

Kendall, M.G., 1938. A new measure of rank correlation. Biometrika 30, 81–93. doi: 10.1093/biomet/30.1-2.81.

Kirchner, J.W., Feng, X., Neal, C., 2001. Catchment-scale advection and dispersion as a mechanism for fractal scaling in stream tracer concentrations. Journal of Hydrology 254, 82–101. doi: 10.1016/s0022-1694(01)00487-5.

Kulmatiski, A., Beard, K.H., 2012. Root niche partitioning among grasses, saplings, and trees measured using a tracer technique. Oecologia 171, 25–37. doi: 10.1007/s00442-012-2390-0.

Kübert, A., Paulus, S., Dahlmann, A., Werner, C., Rothfuss, Y., Orlowski, N., Dubbert, M., 2020. Water Stable Isotopes in Ecohydrological Field Research: Comparison Between In Situ and Destructive Monitoring Methods to Determine Soil Water Isotopic Signatures. Frontiers in Plant Science 11, Article 387. doi: 10.3389/fpls.2020.00387.

Laird, A.K., 1964. Dynamics of Tumor Growth. British Journal of Cancer 18, 490–502. doi: 10.1038/bjc.1964.55.

Lawrence, D.M., Oleson, K.W., Flanner, M.G., Thornton, P.E., Swenson, S.C., Lawrence, P.J., Zeng, X., Yang, Z.L., Levis, S., Sakaguchi, K., Bonan, G.B., Slater, A.G., 2011. Parameterization improvements and functional and structural advances in version 4 of the community land model. Journal of Advances in Modeling Earth Systems 3, M03001. doi: 10.1029/2011ms00045.

Lawrence, M.G., 2005. The Relationship between Relative Humidity and the Dewpoint Temperature in Moist Air: A Simple Conversion and Applications. Bulletin of the American Meteorological Society 86, 225–234. doi: 10.1175/bams-86-2-225.

Leal, S., Sousa, V.B., Knapic, S., Louzada, J.L., Pereira, H., 2011. Vessel size and number are contributors to define wood density in cork oak. European Journal of Forest Research 130, 1023–1029. doi: 10.1007/s10342-011-0487-3.

Leal, S., Sousa, V.B., Pereira, H., 2007. Radial variation of vessel size and distribution in cork oak wood (Quercus suber L.). Wood Science and Technology 41, 339–350. doi: 10.1007/s00226-006-0112-7.

Leibundgut, C., 2009. Tracers in hydrology. Wiley-Blackwell, Chichester, UK Hoboken, NJ.

LI-COR Inc, 2012. Using the LI-6400 / LI-6400XT – Portable Photosynthesis System. version 6 Ed. LI-COR Biosciences Inc, USA.

Lu, N., 2016. Generalized Soil Water Retention Equation for Adsorption and Capillarity. Journal of Geotechnical and Geoenvironmental Engineering 142, 04016051. doi: 10.1061/(asce)gt.1943-5606.0001524.

Mahindawansha, A., Orlowski, N., Kraft, P., Rothfuss, Y., Racela, H., Breuer, L., 2018. Quantification of plant water uptake by water stable isotopes in rice paddy systems. Plant and Soil 429, 281–302. doi: 10.1007/s11104-018-3693-7.

Majoube, M., 1971. Fractionnement en oxygène 18 et en deutérium entre l'eau et sa vapeur. Journal de Chimie Physique 68, 1423–1436. doi: 10.1051/jcp/1971681423.

McDonnell, J.J., 2014. The two water worlds hypothesis: ecohydrological separation of water between streams and trees? Wiley Interdisciplinary Reviews: Water 1, 323–329. doi: 10.1002/wat2.1027.

Meeinzer, F.C., Brooks, J.R., Domec, J.C., Gartner, B.L., Warren, J.M., Woodruff, D.R., Bible, K., Shaw, D.C., 2006. Dynamics of water transport and storage in conifers studied with deuterium and heat tracing techniques. Plant, Cell and Environment 29, 105–114. doi: 10.1111/j.1365-3040.2005.01404.x.

Merlivat, L., Jouzel, J., 1979. Global climatic interpretation of the deuterium-oxygen 18 relationship for precipitation. Journal of Geophysical Research 84, 5029. doi: 10.1029/jc084ic08p05029.

Millar, C., Pratt, D., Schneider, D.J., McDonnell, J.J., 2018. A comparison of extraction systems for plant water stable isotope analysis. Rapid Communications in Mass Spectrometry 32, 1031–1044. doi: 10.1002/rcm.8136.

Oerter, E.J., Perelet, A., Pardyjak, E., Bowen, G., 2016. Membrane inlet laser spectroscopy to measure H and O stable isotope compositions of soil and sediment pore water with high sample throughput. Rapid Communications in Mass Spectrometry 31, 75–84. doi: 10.1002/rcm.7768.

O'Grady, A.P., Eamus, D., Hutley, L.B., 1999. Transpiration increases during the dry season: patterns of tree water use in eucalypt open-forests of northern Australia. Tree Physiology 19, 591–597. doi: 10.1093/treephys/19.9.591.

Oren, R., Pataki, D.E., 2001. Transpiration in response to variation in microclimate and soil moisture in southeastern deciduous forests. Oecologia 127, 549–559. doi: 10.1007/s004420000622.

Orians, C.M., van Vuuren, M.M.I., Harris, N.L., Babst, B.A., Ellmore, G.S., 2004. Differential sectoriality in long-distance transport in temperate tree species: evidence from dye flow, 15n transport, and vessel element pitting. Trees 18, 501–509. doi: 10.1007/s00468-004-0326-y.

Orlowski, N., Breuer, L., Angeli, N., Boeckx, P., Brumbt, C., Cook, C.S., Dubbert, M., Dyckmans, J., Gallagher, B., Gralher, B., Herbstritt, B., Hervé-Fernández, P., Hissler, C., Koeniger, P., Legout, A., Macdonald, C.J., Oyarzún, C., Redelstein, R., Seidler, C., Siegwolf, R., Stumpp, C., Thomsen, S., Weiler, M., Werner, C., McDonnell, J.J., 2018a. Inter-laboratory comparison of cryogenic water extraction systems for stable isotope analysis of soil water. Hydrology and Earth System Sciences 22, 3619–3637. doi: 10.5194/hess-22-3619-2018.

Orlowski, N., Breuer, L., McDonnell, J.J., 2016a. Critical issues with cryogenic extraction of soil water for stable isotope analysis. Ecohydrology 9, 1–5. doi: 10.1002/eco.1722.

Orlowski, N., Frede, H.G., Brüggemann, N., Breuer, L., 2013. Validation and application of a cryogenic vacuum extraction system for soil and plant water extraction for isotope analysis. Journal of Sensors and Sensor Systems 2, 179–193. doi: 10.5194/jsss-2-179-2013.

Orlowski, N., Pratt, D.L., McDonnell, J.J., 2016b. Intercomparison of soil pore water extraction methods for stable isotope analysis. Hydrological Processes 30, 3434–3449. doi: 10.1002/hyp.10870.

Orlowski, N., Winkler, A., McDonnell, J.J., Breuer, L., 2018b. A simple greenhouse experiment to explore the effect of cryogenic water extraction for tracing plant source water. Ecohydrology 11, 1–12. doi: 10.1002/eco.1967.

Pfautsch, S., Bleby, T.M., Rennenberg, H., Adams, M.A., 2010. Sap flow measurements reveal influence of temperature and stand structure on water use of eucalyptus regnans forests. Forest Ecology and Management 259, 1190–1199. doi: 10.1016/j.foreco.2010.01.006.

Pfautsch, S., Renard, J., Tjoelker, M.G., Salih, A., 2015. Phloem as Capacitor: Radial Transfer of Water into Xylem of Tree Stems Occurs via Symplastic Transport in Ray Parenchyma. Plant Physiology 167, 963–971. doi: 10.1104/pp.114.254581.

Poca, M., Coomans, O., Urcelay, C., Zeballos, S.R., Bodé, S., Boeckx, P., 2019. Isotope fractionation during root water uptake by Acacia caven is enhanced by arbuscular mycorrhizas. Plant and Soil 441, 485–497. doi: 10.1007/s11104-019-04139-1.

Rothfuss, Y., Javaux, M., 2017. Reviews and syntheses: Isotopic approaches to quantify root water uptake: a review and comparison of methods. Biogeosciences 14, 2199–2224. doi: 10.5194/bg-14-2199-2017.

Rothfuss, Y., Vereecken, H., Brüggemann, N., 2013. Monitoring water stable isotopic composition in soils using gas-permeable tubing and infrared laser absorption spectroscopy. Water Resources Research 49, 3747–3755. doi: 10.1002/wrcr.20311.

Schepper, V.D., van Dusschoten, D., Copini, P., Jahnke, S., Steppe, K., 2012. MRI links stem water content to stem diameter variations in transpiring trees. Journal of Experimental Botany 63, 2645–2653. doi: 10.1093/jxb/err445.

Sprenger, M., Herbstritt, B., Weiler, M., 2015a. Established methods and new opportunities for pore water stable isotope analysis. Hydrological Processes 29, 5174–5192. doi: 10.1002/hyp.10643.

Sprenger, M., Llorens, P., Cayuela, C., Gallart, F., Latron, J., 2019. Mechanisms of consistently disjunct soil water pools over (pore) space and time. Hydrology and Earth System Sciences 23, 2751–2762. doi: 10.5194/hess-23-2751-2019.

Sprenger, M., Seeger, S., Blume, T., Weiler, M., 2016. Travel times in the vadose zone: Variability in space and time. Water Resources Research 52, 5727–5754. doi: 10.1002/2015wr018077.

Sprenger, M., Volkmann, T.H.M., Blume, T., Weiler, M., 2015b. Estimating flow and transport parameters in the unsaturated zone with pore water stable isotopes. Hydrology and Earth System Sciences 19, 2617–2635. doi: 10.5194/hess-19-2617-2015.

Stumpp, C., Hendry, M.J., 2012. Spatial and temporal dynamics of water flow and solute transport in a heterogeneous glacial till: The application of high-resolution profiles of δ18o and δ2h in pore waters. Journal of Hydrology 438-439, 203–214. doi: 10.1016/j.jhydrol.2012.03.024.

Tuller, M., Or, D., 2005. Water films and scaling of soil characteristic curves at low water contents. Water Resources Research 41, W09403. doi: 10.1029/2005wr004142.

Vandegehuchte, M.W., Steppe, K., 2013. Corrigendum to: Sap-flux density measurement methods: working principles and applicability. Functional Plant Biology 40, 1088. doi: 10.1071/fp12233_co.

Vargas, A.I., Schaffer, B., Yuhong, L., da Silveira Lobo Sternberg, L., 2017. Testing plant use of mobile vs immobile soil water sources using stable isotope experiments. New Phytologist 215, 582–594. doi: 10.1111/nph.14616.

Volkmann, T.H.M., Haberer, K., Gessler, A., Weiler, M., 2016a. High-resolution isotope measurements resolve rapid ecohydrological dynamics at the soil-plant interface. New Phytologist 210, 839–849. doi: 10.1111/nph.13868.

Volkmann, T.H.M., Kühnhammer, K., Herbstritt, B., Gessler, A., Weiler, M., 2016b. A method forin situmonitoring of the isotope composition of tree xylem water using laser spectroscopy. Plant, Cell & Environment 39, 2055–2063. doi: 10.1111/pce.12725.

Volkmann, T.H.M., Weiler, M., 2014. Continual in situ monitoring of pore water stable isotopes in the subsurface. Hydrology and Earth System Sciences 18, 1819–1833. doi: 10.5194/hess-18-1819-2014.

Walker, G.R., Woods, P.H., Allison, G.B., 1994. Interlaboratory comparison of methods to determine the stable isotope composition of soil water. Chemical Geology 111, 297–306. doi: 10.1016/0009-2541(94)90096-5.

Wang, L., Caylor, K.K., Villegas, J.C., Barron-Gafford, G.A., Breshears, D.D., Huxman, T.E., 2010. Partitioning evapotranspiration across gradients of woody plant cover: Assessment of a stable isotope technique. Geophysical Research Letters 37, L09401. doi: 10.1029/2010gl043228.

Wassenaar, L., Hendry, M., Chostner, V., Lis, G., 2008. High Resolution Pore Water δ^2H andδ^{18}O Measurements by H2O(liquid)-H2O(vapor)Equilibration Laser Spectroscopy. Environmental Science & Technology 42, 9262–9267. doi: 10.1021/es802065s.

White, J.W.C., Cook, E.R., Lawrence, J.R., Broecker, W.S., 1985. The ratios of sap in trees: Implications for water sources and tree ring ratios. Geochimica et Cosmochimica Acta 49, 237–246. doi: 10.1016/0016-7037(85)90207-8.

Wigmosta, M.S., Vail, L.W., Lettenmaier, D.P., 1994. A distributed hydrology-vegetation model for complex terrain. Water Resources Research 30, 1665–1679. doi: 10.1029/94wr00436.

Zhao, L., Wang, L., Cernusak, L.A., Liu, X., Xiao, H., Zhou, M., Zhang, S., 2016. Significant Difference in Hydrogen Isotope Composition Between Xylem and Tissue Water *Populus Euphratica*. Plant, Cell & Environment 39, 1848–1857. doi: 10.1111/pce.12753.

Acronyms

	unit	symbol
air temperature	°C or K	T_a
deuterium excess	‰	d
field kapacity	mm	FK
general linear model		GLM
global meteoric water line		GMWL
local meteoric water line		LMWL
mean value		$\overline{x}$
permanent wilting point		PWP
pH-value		pH
photosynthetically active radiation	$\mu mol\,m^{-2}\,s^{-1}$	PAR
precipitation	mm	P
relative humidity	%	RH
root mean square difference		RMSD
sap flow velocity	$cm\,h^{-1}$	V_{sap}
standard deviation		sd
soil moisture tension (pF values)	log cm SMT	pF
soil temperature	°C	T_s
specific heat capacity of water	$J\,m^{-3}\,K^{-1}$	C_w
thermal conductivity	$W\,m^{-1}\,K^{-1}$	k
time	s, min, h, d, y	t
total solar radiation	W	TSI
vapor pressure deficit	kPa	VPD
Vienna Standard Mean Ocean Water		VSMOW
volumetric water content (soil moisture)	%	VWC
water temperature	°C	T_w

Appendix

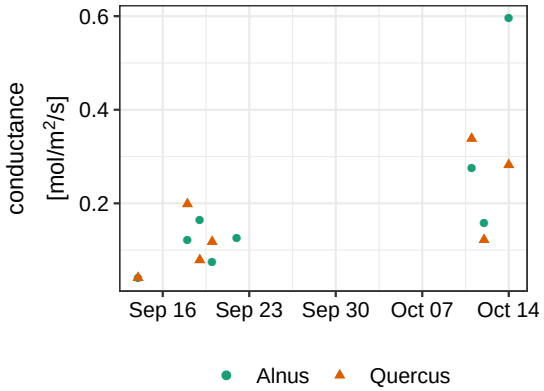

Figure A.1: Maximum leave conductance measured with a portable photosynthesis equipment (LI-COR) around noon.

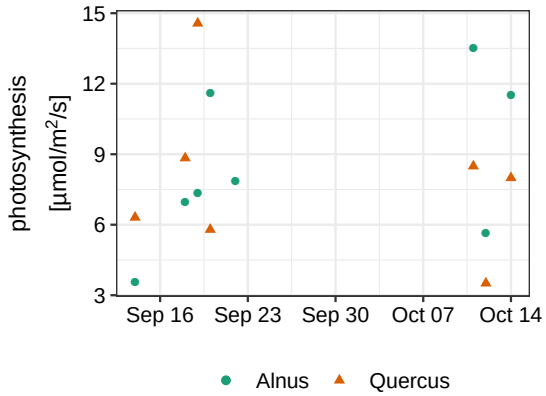

Figure A.2: Maximum photosynthesis rates measured with a portable photosynthesis equipment (LI-COR) around noon.

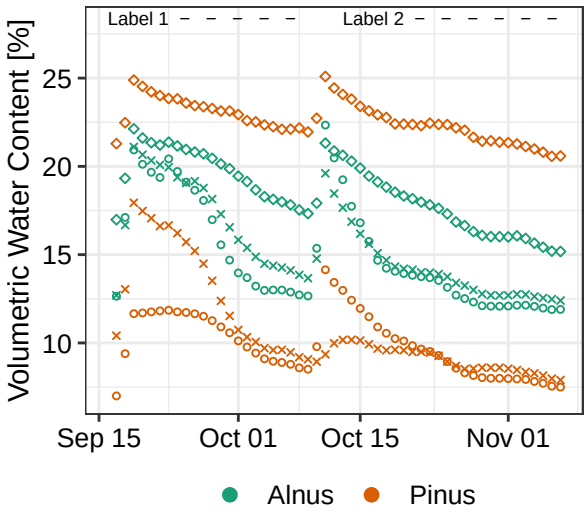

Figure A.3: Daily mean soil moisture (VWC) of root bale (◇) northern (○) and southern (×) soil position in the tree boxes at 30 cm depth. Trees are *Alnus incana* and *Pinus pinea*. *Quercus suber* is excluded because the analysis cannot carried out on this tree due to sap flow velocity sensor failures.

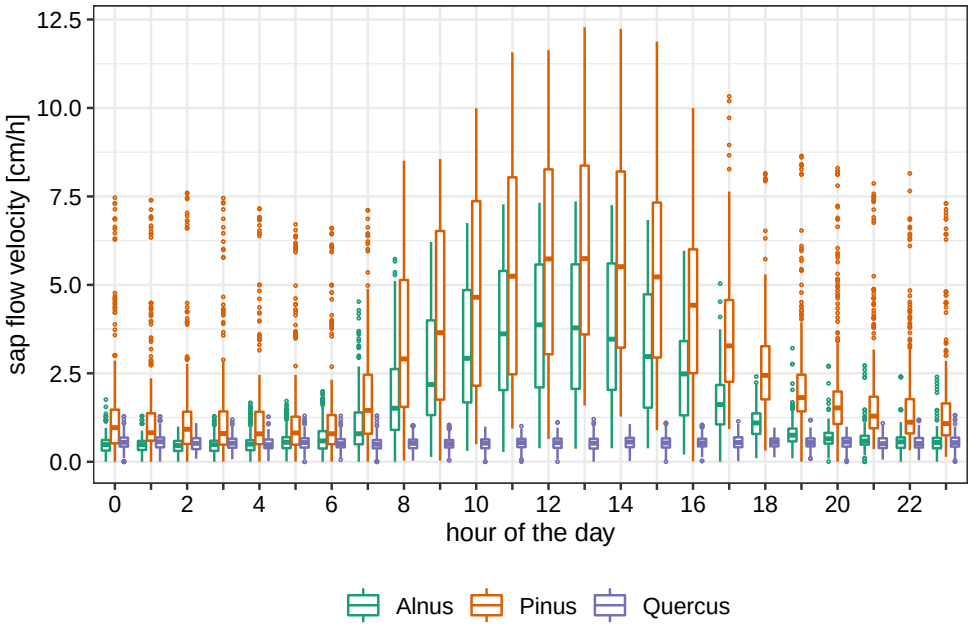

Figure A.4: Sap flow velocities at 150 cm height for *Alnus incana*, *Pinus pinea* and *Quercus suber* grouped in hour of the day via boxplots. Due to the many measurements more outliers (dots) can occur. However, sap flow velocity for *Quercus suber* is influenced by sensor failure and therefore excluded in further results

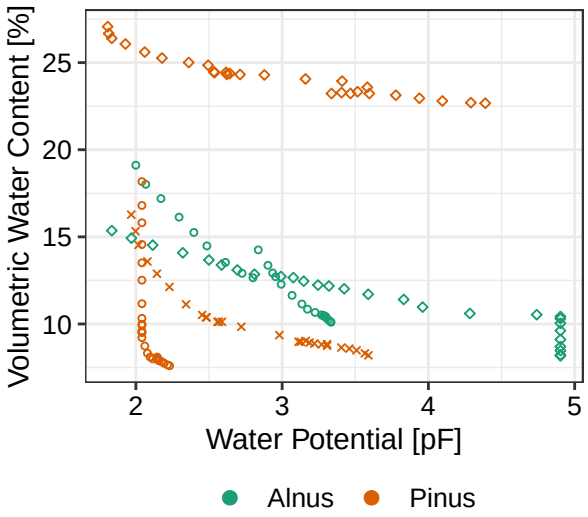

Figure A.5: Correlation between soil moisture (VWC) and soil metric water potential (pF-value) of root bale (◇) northern (○) and southern (×) soil position in the tree boxes at 15 cm depth during the second labelling. Data points are daily mean values. Trees are *Alnus incana* and *Pinus pinea*. *Quercus suber* is excluded because the analysis cannot carried out on this tree due to sap flow velocity sensor failures.

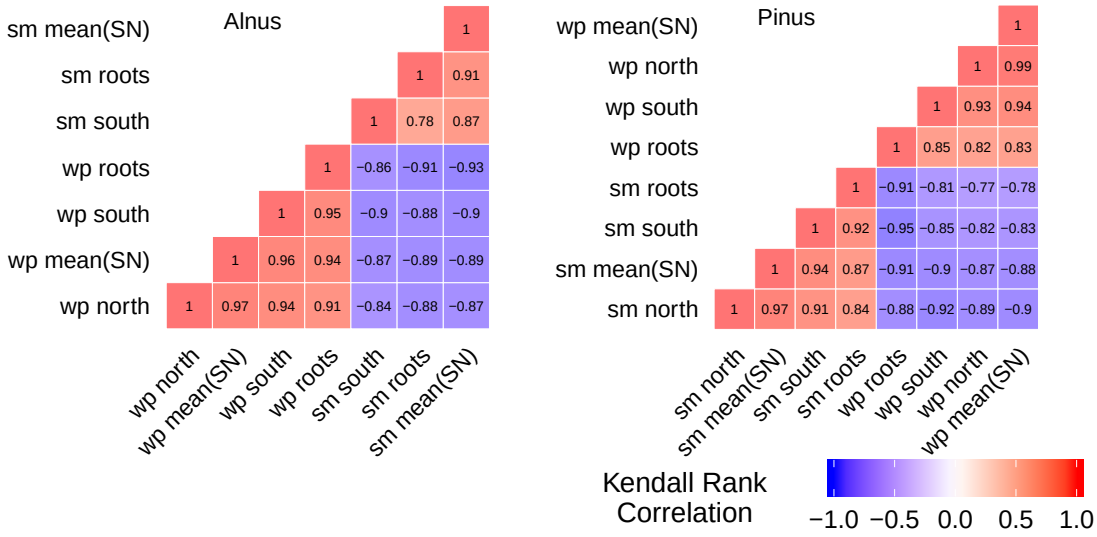

Figure A.6: Kandall rank correlation matrix between soil moisture (sm) and water potential (wp) sensors at 15 cm depth for *Alnus incana* and *Pinus pinea*. Mean (SN) represents the average of southern and northern sensor. Note: for *Alnus incana* one sensor is missing due to failure.

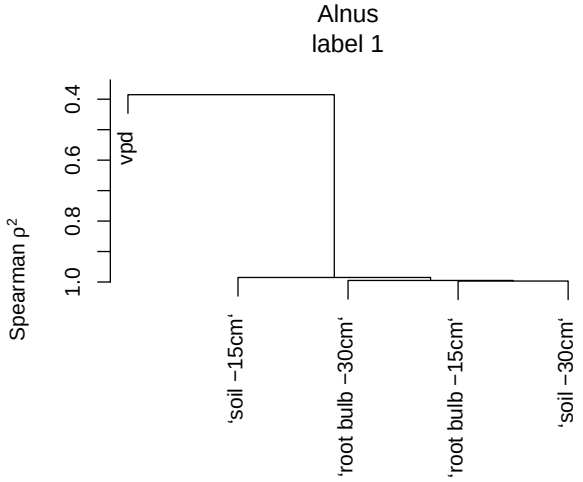

Figure A.7: Results for cluster analysis (Spearman rank correlation) of independent variables of the GLM analysis for *Alnus incana*. Only data after the first labelling and before the second labelling is included.

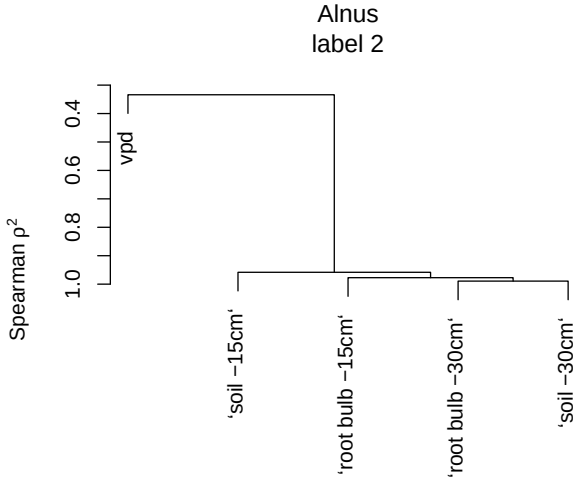

Figure A.8: Results for cluster analysis (Spearman rank correlation) of independent variables of the GLM analysis for *Alnus incana*. Only data after the second labelling is included.

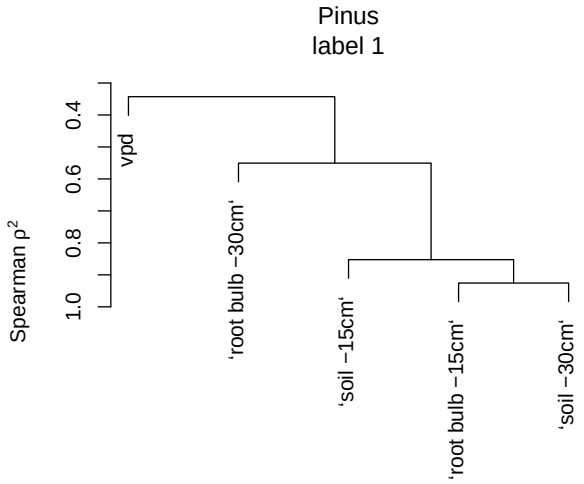

Figure A.9: Results for cluster analysis (Spearman rank correlation) of independent variables of the GLM analysis for *Pinus pinea*. Only data after the first labelling and before the second labelling is included.

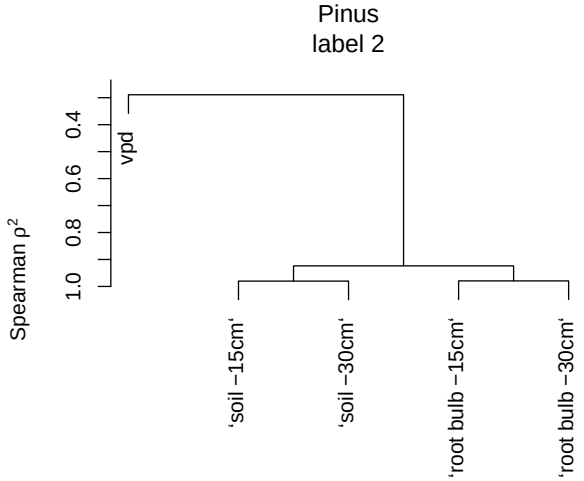

Figure A.10: Results for cluster analysis (Spearman rank correlation) of independent variables of the GLM analysis for *Alnus incana*. Only data after the second labelling is included.

Table A.1: Result of GLMs to analyse influences on the dependent variables (sap flow velocity) by the independent variables corresponding to soil and atmospheric conditions (VPD and soil moistures in 15 cm and 30 cm). GLMs are simplified if possible by using ANOVA to detect significance of independent variables. Furthermore, interactions between independent variables were allowed (symbolised by ":"). The table represents results for *Alnus incana* after the first labelling event but before the second labelling event.

	Dependent variable:	
	sap flow v. 15 cm	sap flow v. 150 cm
	(1)	(2)
VPD	29.992***	28.242***
	(3.700)	(3.793)
soil moisture 15 cm	−0.762	−0.591
	(0.917)	(0.968)
soil moisture 30 cm	2.354**	2.167*
	(1.134)	(1.189)
VPD:soil moisture 15 cm	−1.708***	−1.630***
	(0.220)	(0.229)
Constant	−31.062***	−30.393***
	(8.602)	(9.042)
Observations	65	56
R^2	0.665	0.659
Adjusted R^2	0.642	0.632
Residual Std. Error	1.040 (df = 60)	1.047 (df = 51)
F Statistic	29.733*** (df = 4; 60)	24.599*** (df = 4; 51)
Note:		*p<0.1; **p<0.05; ***p<0.01

Table A.2: Result of GLMs to analyse influences on the dependent variables (sap flow velocity) by the independent variables corresponding to soil and atmospheric conditions (VPD and soil moistures in 15 cm and 30 cm). GLMs are simplified if possible by using ANOVA to detect significance of independent variables. Furthermore, interactions between independent variables were allowed (symbolised by ":"). The table represents results for *Alnus incana* after the second labelling event.

	Dependent variable:	
	sap flow v. 15 cm	sap flow v. 150 cm
	(1)	(2)
VPD	−44.405*	−59.698**
	(25.932)	(22.891)
soil moisture 15 cm	−2.058	−2.884**
	(1.474)	(1.301)
soil moisture 30 cm	0.124	−1.165
	(1.693)	(1.494)
VPD:soil moisture 15 cm	5.006***	5.308***
	(1.836)	(1.620)
VPD:soil moisture 30 cm	2.561	3.561**
	(1.784)	(1.574)
soil moisture 15 cm:soil moisture 30 cm	0.101	0.163*
	(0.103)	(0.091)
VPD:soil moisture 15 cm:soil moisture 30 cm	−0.268**	−0.300***
	(0.109)	(0.096)
Constant	3.230	22.131
	(23.942)	(21.134)
Observations	81	81
R^2	0.906	0.905
Adjusted R^2	0.897	0.896
Residual Std. Error (df = 73)	0.819	0.723
F Statistic (df = 7; 73)	100.960***	99.247***
Note:		*p<0.1; **p<0.05; ***p<0.01

Table A.3: Result of GLMs to analyse influences on the dependent variables (sap flow velocity) by the independent variables corresponding to soil and atmospheric conditions (VPD and soil moistures in 15 cm and 30 cm). GLMs are simplified if possible by using ANOVA to detect significance of independent variables. Furthermore, interactions between independent variables were allowed (symbolised by ":"). The table represents results for *Pinus pinea* after the first labelling event but before the second labelling event.

	Dependent variable:	
	sap flow v. 15 cm	sap flow v. 150 cm
	(1)	(2)
VPD	46.423***	53.523***
	(12.626)	(15.643)
soil moisture 15 cm	19.810***	18.260***
	(5.661)	(6.433)
soil moisture 30 cm	29.993***	31.532***
	(4.856)	(5.157)
VPD:soil moisture 15 cm	0.279	1.088
	(1.475)	(1.680)
VPD:soil moisture 30 cm	−2.215	−3.411
	(2.000)	(2.325)
soil moisture 15 cm:soil moisture 30 cm	−0.981***	−0.969***
	(0.200)	(0.223)
Constant	−615.341***	−618.292***
	(109.087)	(117.878)
Observations	69	59
R^2	0.664	0.696
Adjusted R^2	0.631	0.661
Residual Std. Error	1.234 (df = 62)	1.265 (df = 52)
F Statistic	20.385*** (df = 6; 62)	19.852*** (df = 6; 52)
Note:		*p<0.1; **p<0.05; ***p<0.01

Table A.4: Result of GLMs to analyse influences on the dependent variables (sap flow velocity) by the independent variables corresponding to soil and atmospheric conditions (VPD and soil moistures in 15 cm and 30 cm). GLMs are simplified if possible by using ANOVA to detect significance of independent variables. Furthermore, interactions between independent variables were allowed (symbolised by ":"). The table represents results for *Pinus pinea* after the second labelling event.

	Dependent variable:	
	sap flow v. 15 cm	sap flow v. 150 cm
	(1)	(2)
VPD	45.074***	−904.653***
	(7.862)	(339.247)
soil moisture 15 cm	2.315***	−26.480*
	(0.325)	(14.907)
soil moisture 30 cm		−41.531***
		(11.616)
VPD:soil moisture 15 cm	−1.680***	35.181**
	(0.317)	(15.746)
VPD:soil moisture 30 cm		42.446***
		(15.142)
soil moisture 15 cm:soil moisture 30 cm		1.476***
		(0.555)
VPD:soil moisture 15 cm:soil moisture 30 cm		−1.647***
		(0.604)
Constant	−52.116***	773.785**
	(7.742)	(297.580)
Observations	81	81
R^2	0.772	0.644
Adjusted R^2	0.763	0.610
Residual Std. Error	1.623 (df = 77)	1.962 (df = 73)
F Statistic	86.697*** (df = 3; 77)	18.866*** (df = 7; 73)
Note:		*p<0.1; **p<0.05; ***p<0.01

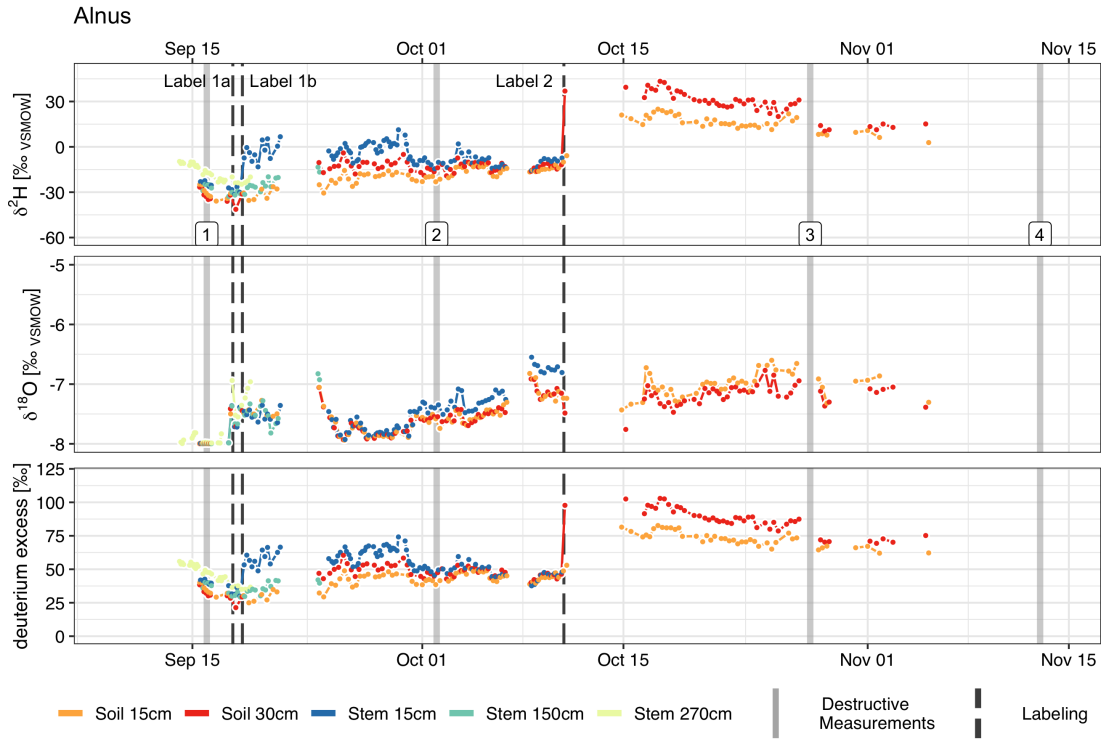

Figure A.11: Isotope measurements with *in-situ* probes in xylem and soil of *Alnus incana* at highest possible temporal resolution (all single measurements). Deuterium and ^{18}O are shown in δ notation while deuterium excess bases on the following equation: $d = \delta\,^{2}H - 8.13 * \delta\,^{18}O$. For reference, plots include destructive measurement campaigns and labelling dates. The connecting lines are interrupted in case of longer time periods than 24 hours in between two measurements.

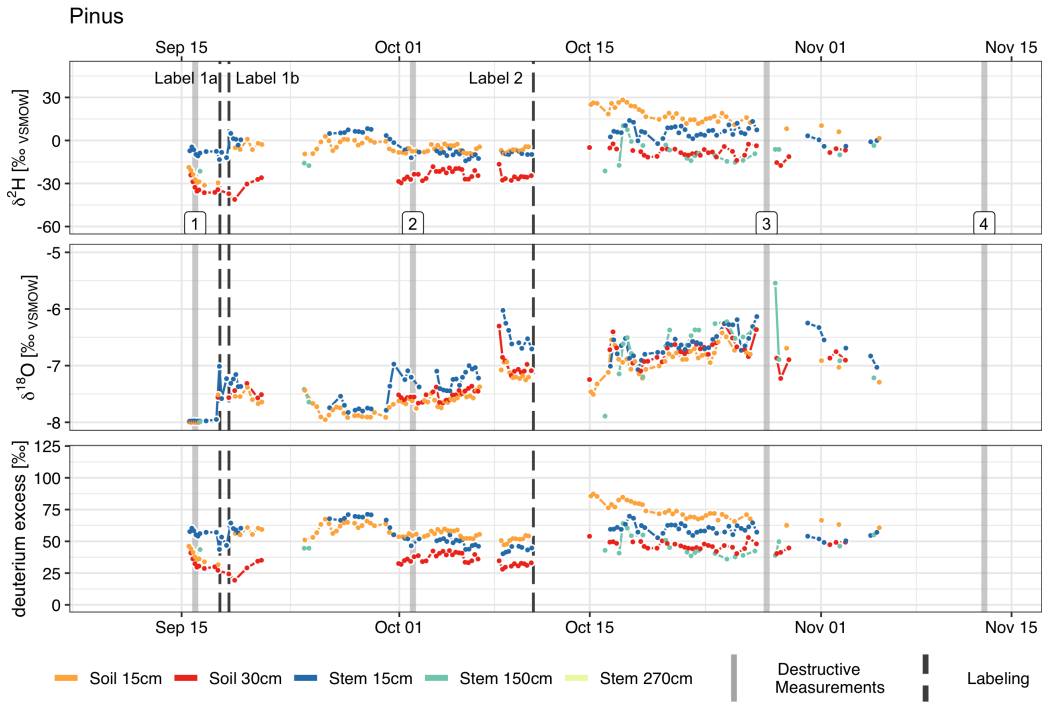

Figure A.12: Isotope measurements with *in-situ* probes in xylem and soil of *Pinus pinea* at highest possible temporal resolution (all single measurements). Deuterium and ^{18}O are shown in δ notation while deuterium excess bases on the following equation: $d = \delta\,^{2}H - 8.13 * \delta\,^{18}O$. For reference, plots include destructive measurement campaigns and labelling dates. The connecting lines are interrupted in case of longer time periods than 24 hours in between two measurements.

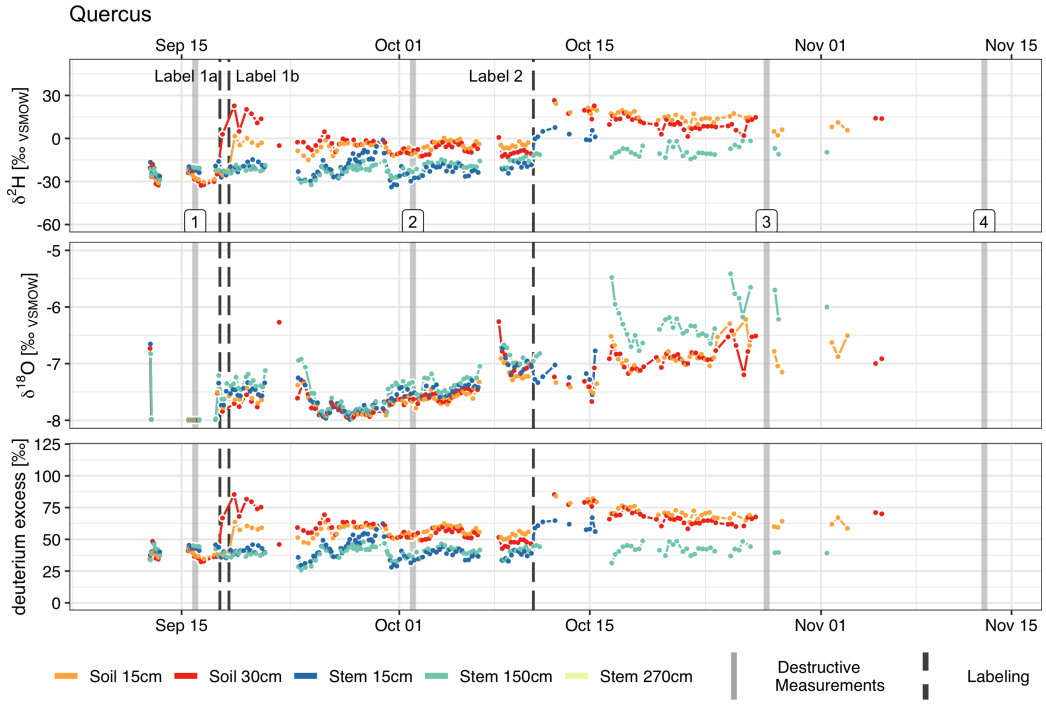

Figure A.13: Isotope measurements with *in-situ* probes in xylem and soil of *Quercus suber* at highest possible temporal resolution (all single measurements). Deuterium and ^{18}O are shown in δ notation while deuterium excess bases on the following equation: $d = \delta\,^{2}H - 8.13 * \delta\,^{18}O$. For reference, plots include destructive measurement campaigns and labelling dates. The connecting lines are interrupted in case of longer time periods than 24 hours in between two measurements.

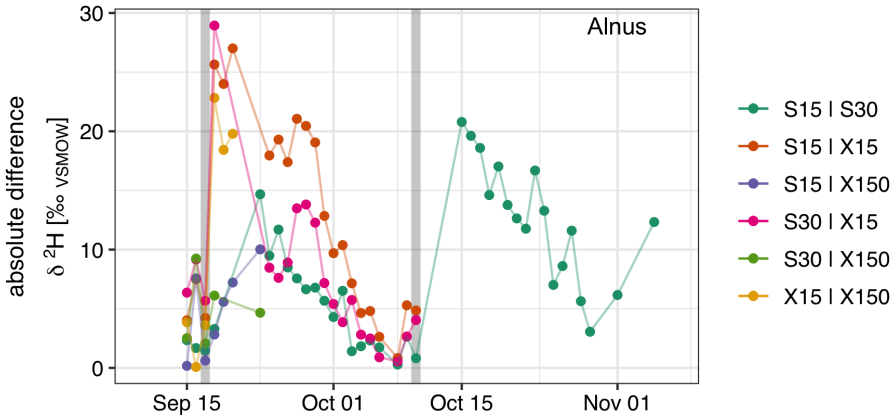

Figure A.14: Absolute differences between δ ^{2}H of different isotope probes in the *Alnus incana* tree pot. Different colors represented combinations of calculated absolute differences between two isotope probes. For reference, grey vertical bars represent the date of labelling.

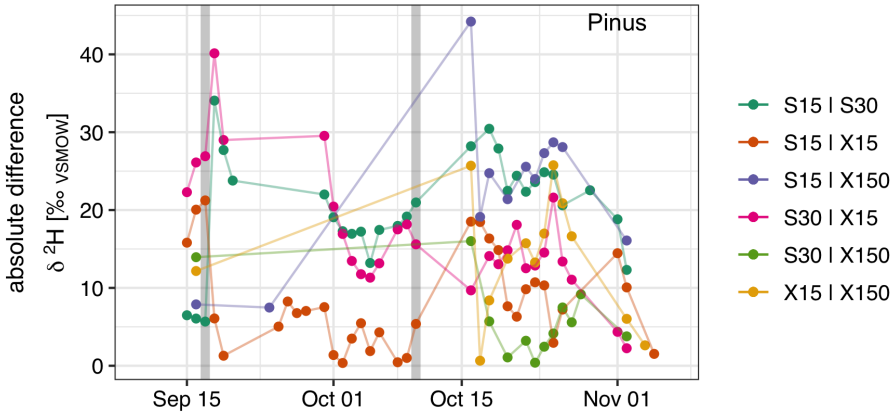

Figure A.15: Absolute differences between δ ^{2}H of different isotope probes in the *Pinus pinea* tree pot. Different colors represented combinations of calculated absolute differences between two isotope probes. For reference, grey vertical bars represent the date of labelling.

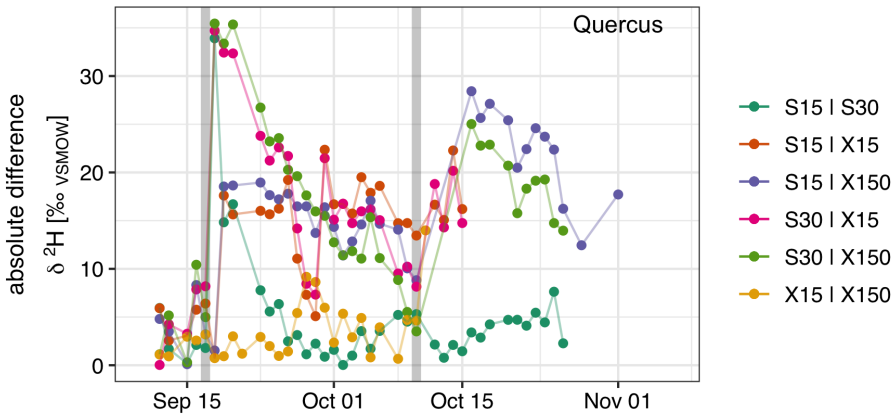

Figure A.16: Absolute differences between δ ^{2}H of different isotope probes in the *Quercus suber* tree pot. Different colors represented combinations of calculated absolute differences between two isotope probes. For reference, grey vertical bars represent the date of labelling.

Table A.5: Schematic tracer response analysis for the second labelling event. Responses for deuterium tracer were calculated by using a visual approach of looking at each single data point. Some isotope probes show clear tracer arrival with the first measurement after tracer application (*) whereas other isotope probes show tracer responses with later measurements (+).

tree	sensor	response delay time and change of δ ^{2}H values in [‰VSMOW]
Alnus	soil 30 cm	within 2 hours*: +39 (-12 -> 37)
Alnus	soil 15 cm	within 5 hours*: +4 (-10 -> -6); (within 4 days$^{+\ -}$: +31)
Alnus	xylem 15 cm	sensor failure
Alnus	xylem 150 cm	sensor failure
Pinus	soil 30 cm	sensor failure
Pinus	soil 15 cm	within 4.5 days$^-$: +29 (-4 -> 25)
Pinus	xylem 15 cm	within 5.5 days$^-$: +12 (-10 -> 2)
Pinus	xylem 150 cm	sensor failure
Quercus	soil 30 cm	within 37 hours*: +37 (-11 -> 26)
Quercus	soil 15 cm	within 40 hours$^+$: +28 (-4 -> 24),
Quercus	xylem 15 cm	within 3 hours*: +20 (-20 -> 0)
Quercus	xylem 150 cm	sensor failure

Note: *first measurement after label; $^+$ not first measurement after label; $^-$ mayor failure

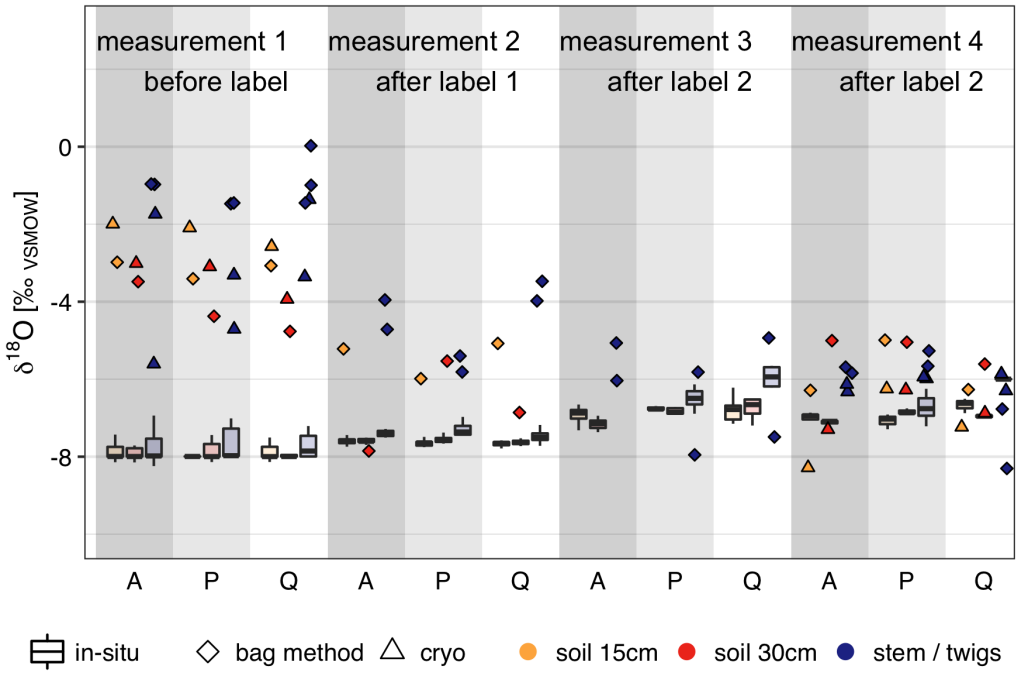

Figure A.17: Comparison of destructive isotope measurement methods (Direct water vapor equilibration = bag method, Cryogenic vacuum extraction = cryo) with *in-situ* isotope measurement for the water isotope ^{18}O in δ notation. Box plots (with median) represent *in-situ* measurements for a three days time frame around the destructive measurement campaigns. Dates of measurement campaigns and applied methods can be found in table 2.4.
Letters at x-axis refer to the trees: A = *Alnus incana*, P = *Pinus pinea*, Q = *Quercus suber*.

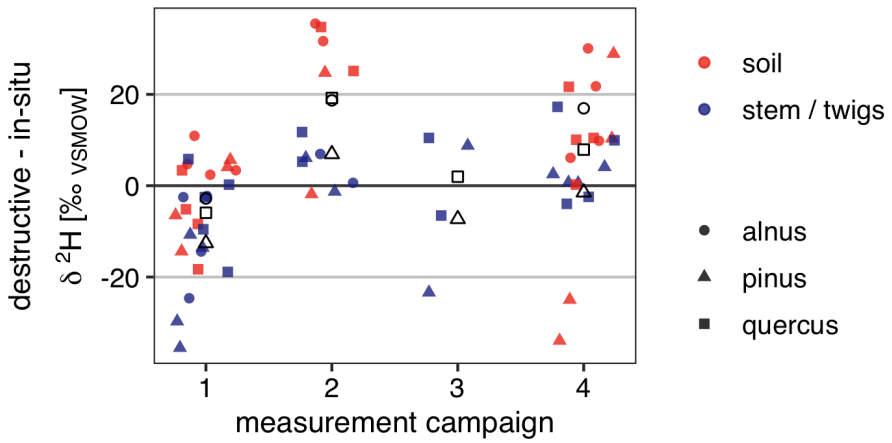

Figure A.18: Differences between destructive and *in-situ* stable isotope measurement methods for δ deuterium values for the four measurement campaigns of destructive sampling. For reference, black hallow points in shape of the tree legend represent median values across all isotopic differences.

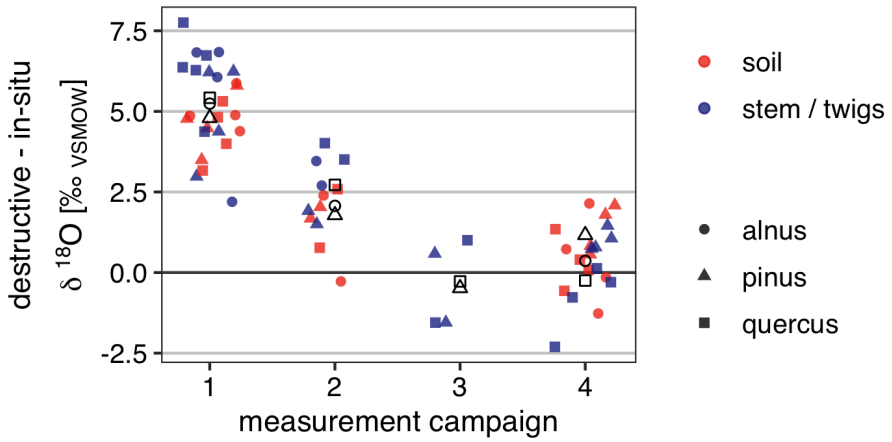

Figure A.19: Differences between destructive and *in-situ* stable isotope measurement methods for δ ^{18}O values for the four measurement campaigns of destructive sampling. For reference, black hallow points in shape of the tree legend represent median values across all isotopic differences.

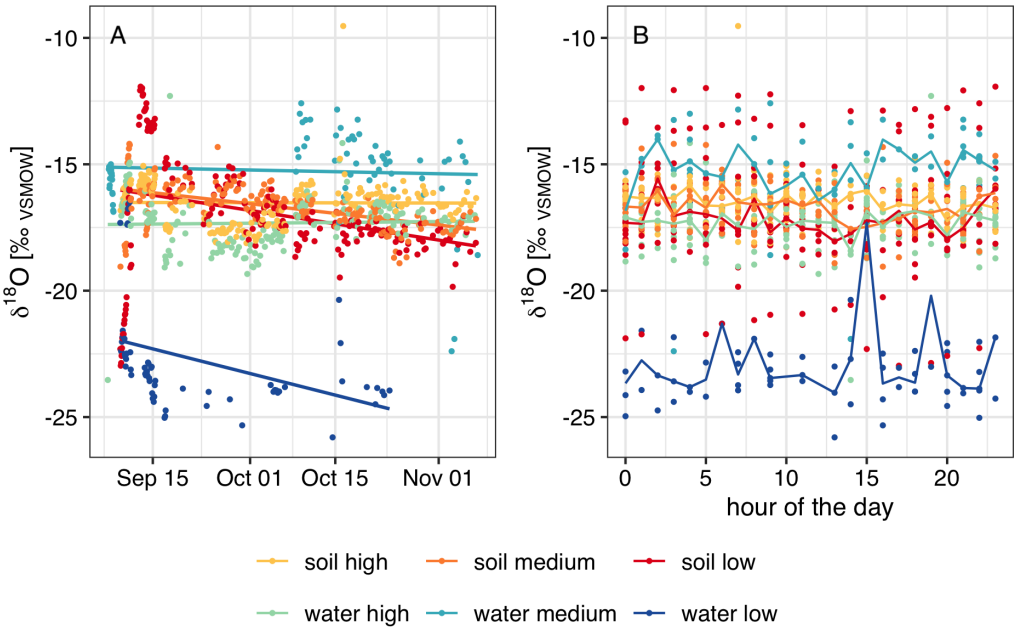

Figure A.20: A: δ ^{18}O values for soil and water standards monitored with *in-situ* isotope probes. The lines indicate the linear trend over the time. Single outlier are not removed because they are less powerful when all standards are used together for transferring soil and xylem probe measurements.
B: Measurements of A grouped according to measurement hour during the day. Lines connect median values for each hour and standard. Note that some hours coincidently contain very few measurements which results in high influences on hourly median value.

Table A.6: Average differences of isotope δ values between averaged soil and xylem probes based on daily median values. Missing values are due to sensor failure. See figure 4.5 for all daily values in a dual isotope plot.

		soil - xylem 15 cm		soil - xylem 150 cm	
time	tree	δ ^{2}H	δ ^{18}O	δ ^{2}H	δ ^{18}O
before labelling	Alnus	-6.16	-0.030	-3.69	-0.046
before labelling	Pinus	-22.10	-0.046	-10.90	-0.078
before labelling	Quercus	-4.72	-0.026	-3.97	-0.047
after label 1	Alnus	-9.80	-0.171	-3.57	-0.106
after label 1	Pinus	-9.62	-0.348		
after label 1	Quercus	16.40	-0.092	16.20	-0.202
after label 2	Alnus				
after label 2	Pinus	-0.91	-0.166	15.00	-0.076
after label 2	Quercus	17.30	-0.209	21.50	-0.598

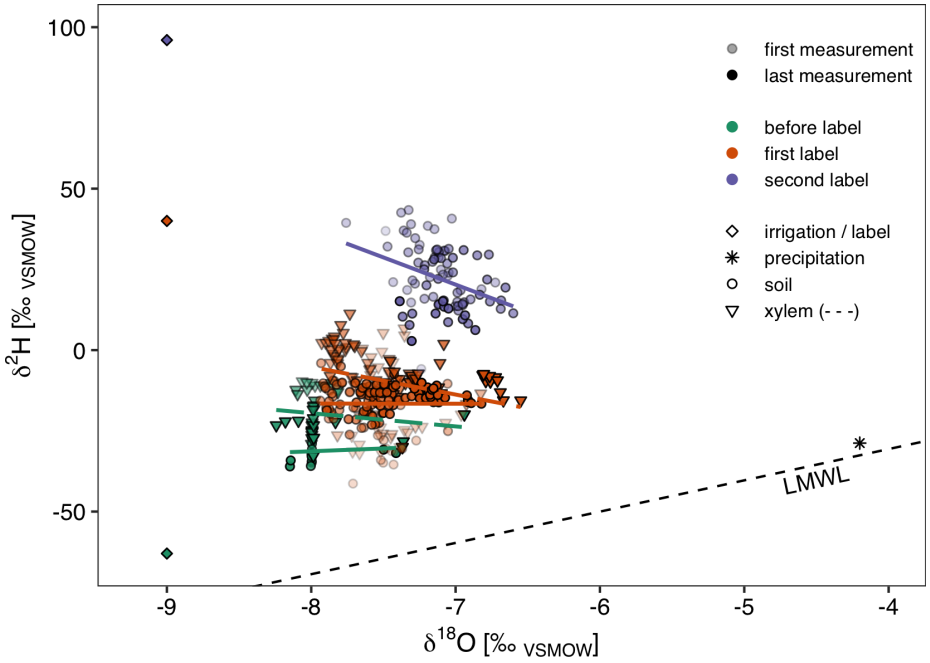

Figure A.21: Stable water isotopes for *Alnus incana* measured by *in-situ* probes shown in dual isotope space. For reference the local meteoric water line (LMWL) and isotopic signal of summer precipitation plus irrigation (shortly before the experiment start) and labelling water are included. Transparency of measurement points corresponds to the time after labelling starting from high transparency with measurements briefly after the labelling.

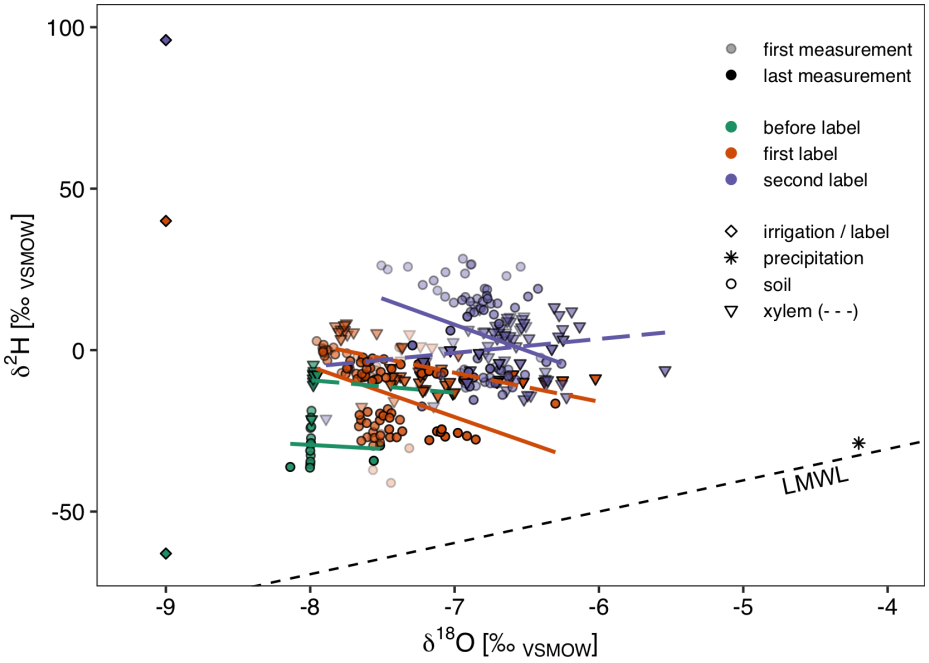

Figure A.22: Stable water isotopes for *Pinus pinea* measured by *in-situ* probes shown in dual isotope space. For reference the local meteoric water line (LMWL) and isotopic signal of summer precipitation plus irrigation (shortly before the experiment start) and labelling water are included. Transparency of measurement points corresponds to the time after labelling starting from high transparency with measurements briefly after the labelling.

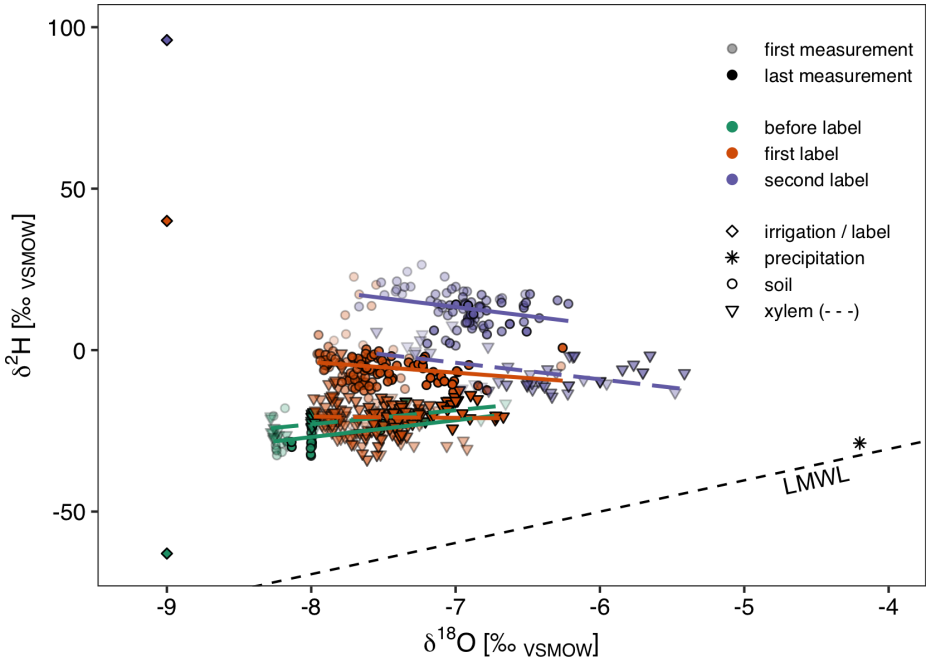

Figure A.23: Stable water isotopes for *Quercus suber* measured by *in-situ* probes shown in dual isotope space. For reference the local meteoric water line (LMWL) and isotopic signal of summer precipitation plus irrigation (shortly before the experiment start) and labelling water are included. Transparency of measurement points corresponds to the time after labelling starting from high transparency with measurements briefly after the labelling.

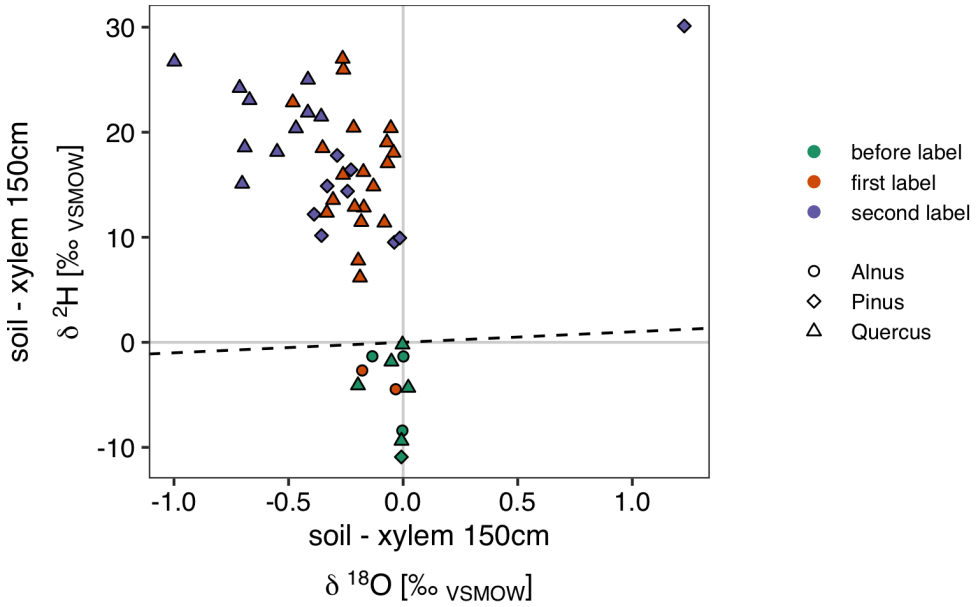

Figure A.24: Differences between measured stable water isotopes in soil (averaged over both probes) and the upper xylem probe in 150 cm stem height shown in dual isotope space. For reference, dashed line indicates 1:1 line.

Ehrenwörtliche Erklärung

Hiermit erkläre ich, dass die Arbeit selbständig und nur unter Verwendung der angegebenen Hilfsmittel angefertigt wurde.

Freiburg i.Br., June 9, 2020

David Johannes Mennekes